AD_____

Award Number: DAMD17-98-1-8102

TITLE: Regulation of Apoptosis by Caspases

PRINCIPAL INVESTIGATOR: Junying Yuan, Ph.D.

CONTRACTING ORGANIZATION: Harvard University
Cambridge, Massachusetts 02138-3800

REPORT DATE: September 1999

TYPE OF REPORT: Annual

PREPARED FOR: U.S. Army Medical Research and Materiel Command
Fort Detrick, Maryland 21702-5012

REPORT DOCUMENTATION PAGE

Form Approved
OMB No. 074-0188

1. AGENCY USE ONLY (Leave blank)	2. REPORT DATE	3. REPORT TYPE AND DATES COVERED
	September 1999	Annual (01 Sep 98 - 31 Aug 99)

4. TITLE AND SUBTITLE
Regulation of Apoptosis by Caspases

5. FUNDING NUMBERS
DAMD17-98-1-8102

6. AUTHOR(S)
Junying Yuan, Ph.D.

7. PERFORMING ORGANIZATION NAME(S) AND ADDRESS(ES)
Harvard University
Cambridge, Massachusetts 02138-3800

e-mail:
jyuan@hms.harvard.edu

8. PERFORMING ORGANIZATION REPORT NUMBER

9. SPONSORING / MONITORING AGENCY NAME(S) AND ADDRESS(ES)
U.S. Army Medical Research and Materiel Command
Fort Detrick, Maryland 21702-5012

10. SPONSORING / MONITORING AGENCY REPORT NUMBER

11. SUPPLEMENTARY NOTES
This report contains colored photos

12a. DISTRIBUTION / AVAILABILITY STATEMENT
Approved for public release ;
distribution unlimited

12b. DISTRIBUTION CODE

13. ABSTRACT ***(Maximum 200 Words)***
Caspases are a family of cysteine proteases that play important roles in regulating apoptosis, a genetically encoded cellular suicide mechanism. To determine the mechanism by which caspases regulate apoptosis. We carried out a screen to identify substrates of caspases using small pool expression cloning method. We have screened 1700 pools which contains approximately 70,000 cDNA clones. From such screening, we identified more than 60 caspase substrates, 10 of which have been verified to be cleaved in vivo during apoptosis. Of these substrates, 24 have not been previously identified or have no assigned function. During the last granting period, we concentrated on characterization of one of the substrates, Bid, which was originally identified as the Bcl-2 interacting protein. We found that Bid is a specific substrate for caspase-8 and is cleaved during Fas and TNF induced apoptosis. Cleaved Bid acts as an intracellular signal transducer from cytoplasmic membrane to mitochondria to induce cytochrome c release. We have also collaborated with Dr. Gerhard Wagner's lab to determine the NMR solution structure of Bid which revealed the structure basis of Bid's action in inducing mitochondrial damage. These works have been published in two papers in *Cell*.

14. SUBJECT TERMS	15. NUMBER OF PAGES
Breast Cancer	29
	16. PRICE CODE

17. SECURITY CLASSIFICATION OF REPORT	18. SECURITY CLASSIFICATION OF THIS PAGE	19. SECURITY CLASSIFICATION OF ABSTRACT	20. LIMITATION OF ABSTRACT
Unclassified	Unclassified	Unclassified	Unlimited

NSN 7540-01-280-5500

Standard Form 298 (Rev. 2-89)
Prescribed by ANSI Std. Z39-18
298-102

FOREWORD

Opinions, interpretations, conclusions and recommendations are those of the author and are not necessarily endorsed by the U.S. Army.

____ Where copyrighted material is quoted, permission has been obtained to use such material.

____ Where material from documents designated for limited distribution is quoted, permission has been obtained to use the material.

____ Citations of commercial organizations and trade names in this report do not constitute an official Department of Army endorsement or approval of the products or services of these organizations.

JY In conducting research using animals, the investigator(s) adhered to the "Guide for the Care and Use of Laboratory Animals," prepared by the Committee on Care and use of Laboratory Animals of the Institute of Laboratory Resources, national Research Council (NIH Publication No. 86-23, Revised 1985).

____ For the protection of human subjects, the investigator(s) adhered to policies of applicable Federal Law 45 CFR 46.

JY In conducting research utilizing recombinant DNA technology, the investigator(s) adhered to current guidelines promulgated by the National Institutes of Health.

JY In the conduct of research utilizing recombinant DNA, the investigator(s) adhered to the NIH Guidelines for Research Involving Recombinant DNA Molecules.

JY In the conduct of research involving hazardous organisms, the investigator(s) adhered to the CDC-NIH Guide for Biosafety in Microbiological and Biomedical Laboratories.

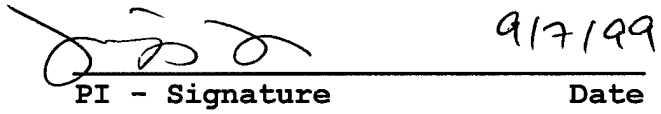

9/7/99

PI - Signature Date

Table of Contents

(5) **Introduction.**

Apoptosis, or programmed cell death, is essential for animal development and tissue homeostasis. Malfunction of this cell-intrinsic suicide pathway may result in cancer, neurodegenerative diseases, or other pathological conditions. Genetic studies in *Caenorhabditis elegans* have revealed two essential components of the apoptotic machinery: CED-3, a cysteine protease, and CED-4, an adapter protein that binds CED-3. In addition, CED-9 protein is an inhibitor of CED-3- and CED-4-mediated apoptosis. The basic apoptotic apparatus and its regulation are evolutionarily conserved, but they have also undergone diversification. Thus, in mammalian cells, members of the Bcl-2 family of proteins are the homologs of CED-9, and either promote or inhibit apoptosis. Apaf-1 is the mammalian homolog of CED-4. Like CED-3, its mammalian homologs, termed caspases, are cysteine proteases that catalyze the cleavage of target proteins at sites downstream of specific aspartic acid residues (see review by Cryns and Yuan, 1998[1]). Although caspases share sequence and other structural similarities, they exhibit different substrate specificities and perform distinct functions. Most caspases are synthesized as proenzymes and are activated by proteolytic processing. Caspase cascades have been implicated in both the initiation and execution of apoptosis. The best characterized apoptosis pathway is that triggered by activation of the Fas receptor. This pathway contributes to the deletion of unwanted mature T cells, cytotoxic T lymphocyte-mediated cytotoxicity, immune privilege, and autoimmune diseases. Cross-linking of the Fas receptor by engagement of the Fas ligand results in formation of the so-called death-inducing signal complex (DISC), which consists of the adapter protein FADD (also known as MORT1) and caspase-8. The formation of DISC leads to the activation of caspase-8; the activated protease then further activates caspases-3, -6, and -7, resulting in mitochondrial damage and cell death. Mouse embryos in which the caspase-8 gene has been inactivated by homologous recombination show defects not only in apoptosis mediated by Fas or by other tumor necrosis factor receptor or nerve growth factor receptor family members, but also in heart muscle development, suggesting that caspase-8 also contributes to developmental processes outside of the immune system.

Mitochondria play important roles in apoptotic signal transduction pathways. Thus, during apoptosis, mitochondria undergo swelling, disruption of their outer membrane, depolarization, and the release of cytochrome c. Cytochrome c release triggers the interaction of Apaf-1 with caspase-9, which, in turn, results in the activation of caspase-9. Activated caspase-9 then cleaves and activates caspase-3, an event that leads to the cleavage of other death substrates and cell death. Bcl-2 and Bcl-x_L inhibit apoptosis by preventing these structural and biochemical changes in mitochondria. However, the upstream inducer of mitochondrial damage remains largely unknown.

Activation of Fas receptor by either ligand binding or antibody crosslinking lead to formation of death inducing signaling complex (DISC) and activation of caspases. Down regulation of Fas has recently been implicated in the breast cancer progression. Keane et al. [2] reported that while nontransformed mammary epithelial cell lines all expressed high levels of Fas mRNA and protein and sensitive to anti-Fas antibody induced apoptosis, only one of seven breast cancer cells expressed high levels of Fas and was sensitive to Fas induced apoptosis. Most of the Fas-resistant cancer cell lines became sensitive to Fas upon interferon-γ (IFN-γ) treatment. Although expression of Fas

is not changed in these IFN-γ treated cells, the expression of ICE is induced. These results suggest that loss of Fas receptor expression may be an important step in breast cancer development and modulation of caspase expression may be of therapeutic value to breast cancer treatment.

(6) **Body**.

The goal of proposed work is to identify the substrates and inhibitors of caspase-2 and caspase-8 using a newly developed small pool expression screening method. We have carried out an extensive screen for caspase-2 and caspase-8. The screen for caspase-8 substrates was very successful (see below), while the screen for caspase-2 substrates was not successful: we have not found a bona fide substrate for caspase-2 so far. It is possible that caspase-2 has very limited substrate specificity and additional study is needed to determine its specificity.

Since caspase-8 is a critical mediator of Fas/TNF induced apoptosis and may play a yet undefined role in embryonic development, we have systematically screened for substrates of caspase-8 with the use of in vitro expression cloning. Screening of about 1700 small pools of cDNAs (100 clones per pool) has resulted in the detection of more than 60 in vitro substrates, 10 of which have been verified to be cleaved in vivo. Of these various proteins, 24 have not been previously identified or have no assigned function. One of the caspase-8 substrates identified is BID, a BH3 (Bcl-2 homolog 3) domain-containing pro-apoptotic member of the Bcl-2 family. Whereas full-length BID is localized in the cytosol and induces only minimal cell death when overexpressed, caspase-8-cleaved BID translocates to the mitochondria and efficiently induces mitochondrial damage and cell death. Thus, BID is an intracellular transducer of the Fas death signal as it travels from the cell membrane to mitochondria. This work has been published in Li et al. [3] (1999). For detail description of the discovery, please refer to the Appendices I. To determine the functional domain required by Bid to induce cytochrome c release from mitochondria, we carried out a mutational analysis of BH3 domain of Bid. Such analysis showed that disruption of Bcl-xL interacting domain in Bid is not sufficient to completely eliminate the ability of Bid to induce apoptosis, and has no effect on truncated Bid to translocate to the mitochondria. Such analysis suggests that Bid may have two structurally separatable functional domains that both contribute to the apoptosis inducing capability of Bid. This hypothesis was supported by the solution structural data (see below).

To determine the structural basis of Bid in inducing cytochrome c release, we collaborated with Dr. Gerhard Wagner's lab to determine the solution structure of Bid by NMR. Such analysis showed that Bid consists of eight alpha helices arranged in a compact fold homologous to Bcl-xL where two central hydrophobic helices are surrounded by six amphipathic helices. Overall structure of Bid is preserved after cleavage by caspase-8; however, such cleavage would expose the two central alpha helices and make the BH3 domain more accessible to the interaction with Bcl-xL. This work was published in Cell (Chou et al. 1998. [4] See Appendices).

Mutational analysis of truncated BID

Mutations of mBid BH3

	L	A	Q	I	G	D	E	M	D
wt									
mt1	G	-	-	-	-	-	-	-	-
mt2	-	-	-	-	-	-	-	A	A
mt3	-	-	-	-	A	-	-	-	-
mt4	-	-	-	-	E	-	-	-	-

	wt	mt1	mt2	mt3	mt4
Apoptosis-inducing activity (Nuclear condensation)	100%	15%	98%	92%	64%
Bcl-x_L binding activity (in vitro)	+++	+	+/-	+++	-
Bcl-x_L binding activity (in vivo)	+++	+	+/-	+++	-
Cyto c releasing activity (immunostaining)	+	+/-	+	+	+
Mitochondrial targeting	+	+	+	+	+

Figure 1. Mutational analysis of Bid. Truncated Bid (starting from a.a.60 to mimic the cleavage product by caspase-8) mutants were generated by site-directed mutagenesis. The ability of such mutants to induce apoptosis, to bind Bcl-xL in vivo and in vitro, to induce cytochrome c release in cells and to translocate to mitochondria were tested individually and scored relative to the wild type truncated Bid.

(7) **Key Research Accomplishments.**

1. Identification of Bid as a key intracellular mediator of Fas/TNF induced apoptosis.

2. Elucidation of structural basis of Bid's action in inducing apoptosis.

(8) **Reportable Outcomes.**

Li H, Zhu H, Xu C-J, and Yuan J. Cleavage of BID by caspase 8 mediates the mitochondrial damage in the Fas pathway of apoptosis. Cell. 1998. 94, 491-501.

Chou JJ, Li H, Salveson G, Yuan J and Wagner G. Solution structure of Bid, an intracellular amplifier of apoptosis. 1999. Cell. 96, 615-624.

(9) **Conclusions.**

We have demonstrated that the small pool expression cloning is an effective method to identify important caspase substrates which will further illustrate the signal

transduction pathway of apoptosis. We have shown that Bid is an important intracellular mediator of Fas/TNF induced apoptosis and a missing link from membrane death receptor signaling to mitochondrial damage. We have identified more than 60 substrates of caspase-8. We have selected a number of them for our future work. We are certain that our work will provide further insight into the mechanism of caspase signal transduction process and such knowledge may allow us to identify critical apoptosis regulators which may allow us to develop effective therapies for breast cancer.

(10) **References**.

1. V. L. Cryns and J. Yuan. Proteases to die for. **Gen. & Dev.** *12*, 1551-1570. (1998).

2. M. M. Keane, et al. Fas expression and function in normal and malignant breast cell lines. *Cancer Research* **56**:4791-8. (1996).

3. H. Li, H. Zhu, C-J Xu, and J. Yuan. Cleavage of BID by caspase 8 mediates the mitochondrial damage in the Fas pathway of apoptosis. **Cell**. *94*, 491-501. (1998).

4. Chou JJ, Li H, Salveson G, Yuan J and Wagner G. Solution structure of Bid, an intracellular amplifier of apoptosis. *Cell.* **96**, 615-624. (1999).

(11) **Appendices**.

I. Li H, Zhu H, Xu C-J, and Yuan J. Cleavage of BID by caspase 8 mediates the mitochondrial damage in the Fas pathway of apoptosis. Cell. 1998. 94, 491-501.

II. Chou JJ, Li H, Salveson G, Yuan J and Wagner G. Solution structure of Bid, an intracellular amplifier of apoptosis. 1999. Cell. 96, 615-624.

Cell, Vol. 94, 491–501, August 21, 1998, Copyright ©1998 by Cell Press

Appendix 1

Cleavage of BID by Caspase 8 Mediates the Mitochondrial Damage in the Fas Pathway of Apoptosis

Honglin Li, Hong Zhu, Chi-jie Xu, and Junying Yuan*
Department of Cell Biology
Harvard Medical School
Boston, Massachusetts 02115

Summary

We report here that BID, a BH3 domain–containing proapoptotic Bcl2 family member, is a specific proximal substrate of Casp8 in the Fas apoptotic signaling pathway. While full-length BID is localized in cytosol, truncated BID (tBID) translocates to mitochondria and thus transduces apoptotic signals from cytoplasmic membrane to mitochondria. tBID induces first the clustering of mitochondria around the nuclei and release of cytochrome c independent of caspase activity, and then the loss of mitochondrial membrane potential, cell shrinkage, and nuclear condensation in a caspase-dependent fashion. Coexpression of $Bclx_L$ inhibits all the apoptotic changes induced by tBID. Our results indicate that BID is a mediator of mitochondrial damage induced by Casp8.

Introduction

Caspase 8 (Casp8), a member of a mammalian caspase family, has been demonstrated to play a key role in mediating Fas-induced apoptosis (Boldin et al., 1996; Fernandes-Alnemri et al., 1996; Muzio et al., 1996; Cryns and Yuan, 1998). Cross-linking of the Fas receptor by engagement of the Fas ligand or agonistic antibodies results in the formation of so-called death-inducing signal complex (DISC), which includes adaptor protein FADD/MORT-1 and Casp8 (Kischkel et al., 1995). The formation of the DISC leads to the activation of Casp8, an initiator of the downstream apoptotic process that includes the activation of Casp3, −6, and −7 and mitochondrial damage (Salvesen and Dixit, 1997). Recently, Scaffidi et al. (1998) have shown that there may be two alternative Fas signaling pathways. In so-called Fas type I cells, a relatively large amount of Casp8 is recruited to DISC upon receptor cross-linking. The activated Casp8 propagates the apoptotic signal by activating downstream caspases through proteolytic cleavage, as well as by triggering mitochondrial damages that in turn activate a proteolytic cascade. In so-called Fas type II cells, a small amount of Casp8 is recruited to the DISC upon receptor cross-linking, and activated Casp8 mediates downstream apoptotic events mainly through inducing mitochondrial damage. These studies, however, did not reveal how active Casp8 induces mitochondrial damage.

A critical role of mitochondria in mediating apoptotic signal transduction pathway has been demonstrated recently (Vander Heiden et al., 1997). Biochemical and structural changes of mitochondria in apoptosis include mitochondrial swelling, disruption of mitochondrial outer membrane, mitochondrial depolarization, and the release of cytochrome c (Liu et al., 1996; Vander Heiden et al., 1997). The release of cytochrome c may trigger the interaction of Apaf1, a mammalian CED-4 homolog, and Casp9, which in turn results in the activation of Casp9 (Li et al., 1997c; Zou et al., 1997). Activated Casp9 then cleaves and activates pro-Casp3, an event that leads to the cleavage of other death substrates, cellular and nuclear morphological changes, and ultimately, cell death. An active site mutant of Casp9 (C287A) is able to block activation of Casp3 by Casp9 (Li et al., 1997c). Overexpression of $Bcl2/Bclx_L$ has been shown to block all apoptosis-induced mitochondrial changes (Kluck et al., 1997; Vander Heiden et al., 1997; Yang et al., 1997). Since mitochondrial damage is an obligatory step in mediating the Fas signaling in type II but not type I cells, $Bcl2/Bclx_L$ can inhibit Fas-induced apoptosis in type II but not type I cells (Scaffidi et al., 1998).

Bcl2 and $Bclx_L$, two members of the Bcl2 family, prevent apoptosis induced by a variety of death stimuli (Merry and Korsmeyer, 1997). They are localized mainly to the outer mitochondrial, nuclear membranes and endoplasmic reticular membrane through their carboxy-terminal membrane anchorage domains. Both of them contain the Bcl2 homology domains designated BH1, BH2, BH3, and BH4, all of which are essential for the antiapoptotic activity of $Bcl2/Bclx_L$ (Merry and Korsmeyer, 1997; Huang et al., 1998). The Bcl2 family also includes a class of BH3 domain–containing death agonists, which may promote apoptosis by inhibiting the death antagonist members of the Bcl2 family (Merry and Korsmeyer, 1997). Mutational analyses indicate that the BH3 domain of death agonists is required for their proapoptotic activity and their interactions with $Bcl2/Bclx_L$ (Chittenden et al., 1995; Wang et al., 1996; Kelekar et al., 1997). It was recently reported that in a cell-free *Xenopus* oocyte system, the BH3 domain alone can induce cytochrome c release and the activation of caspases that can be inhibited by Bcl2 (Cosulich et al., 1997). Thus, these BH3-containing death agonists may play an important regulatory role in mediating apoptotic mitochondrial damage. It is not clear, however, how these BH3 domain–containing proteins fit into the signal transduction pathway of apoptosis and how they act to induce mitochondrial damage.

In this study, we demonstrate that BID, a death agonist member of the $Bcl2/Bclx_L$ family (Wang et al., 1996), is a specific proximal substrate of Casp8 in the Fas signaling pathway. Cleavage of BID by Casp8 releases its potent proapoptotic activity, which in turn induces mitochondrial damage and, ultimately, cell shrinkage and nuclear condensation. Expression of $Bclx_L$ inhibits all the apoptotic phenotypes induced by truncated BID (tBID), whereas caspase inhibitors inhibit the loss of mitochondrial membrane potential, cell shrinkage, and nuclear condensation, but not mitochondrial clustering and cytochrome c release. Our study identified the first specific proximal substrate of Casp8 in the Fas pathway and a critical missing link between the activation of Casp8 and mitochondrial damage.

*To whom correspondence should be addressed.

Results

BID Is a Specific Substrate of Caspase 8 In Vitro

To identify the substrates of Casp8, we transcribed and translated in vitro a small pool mouse spleen cDNA library in the presence of ^{35}S-methionine, using the methods of Lustig et al. (1997). The radioactively labeled protein pools were incubated with either recombinant Casp8 in bacterial lysates or control lysates and analyzed by SDS-PAGE. cDNA small pools (1700) were screened, and the individual cDNA clones containing candidate Casp8 substrates were isolated from positive pools. In pool #814, a 24 kDa protein disappeared after incubation with Casp8 (Figure 1A). This pool was subdivided, and the cDNA encoding this 24 kDa protein was isolated and sequenced. The 24 kDa protein was identified to be murine BID, a proapoptotic Bcl2 family member whose homology to other members of the family is limited to a BH3 domain (Wang et al., 1996). N-terminal T7-tagged BID was cleaved by Casp8 into 15 kDa and 14 kDa fragments in vitro (due to the different contents of methionine in these two fragments, the two ^{35}S-Met-labeled fragments did not appear to be stoichiometric) (Figure 1B). As the majority of the caspase substrates identified so far are the substrates of Casp3, we determined the specificity of BID cleavage by Casp3 and −8, using PARP as a control. ^{35}S-labeled proteins were incubated with limited amounts of Casp3 and −8 for different lengths of time, and the cleavage efficiencies were evaluated by SDS-PAGE. As shown in Figure 1B, Casp8 cleaved most of BID but very little of PARP in 15 min, while the contrary was true for Casp3. This in vitro cleavage result indicates that BID is a much better substrate of Casp8 than of Casp3.

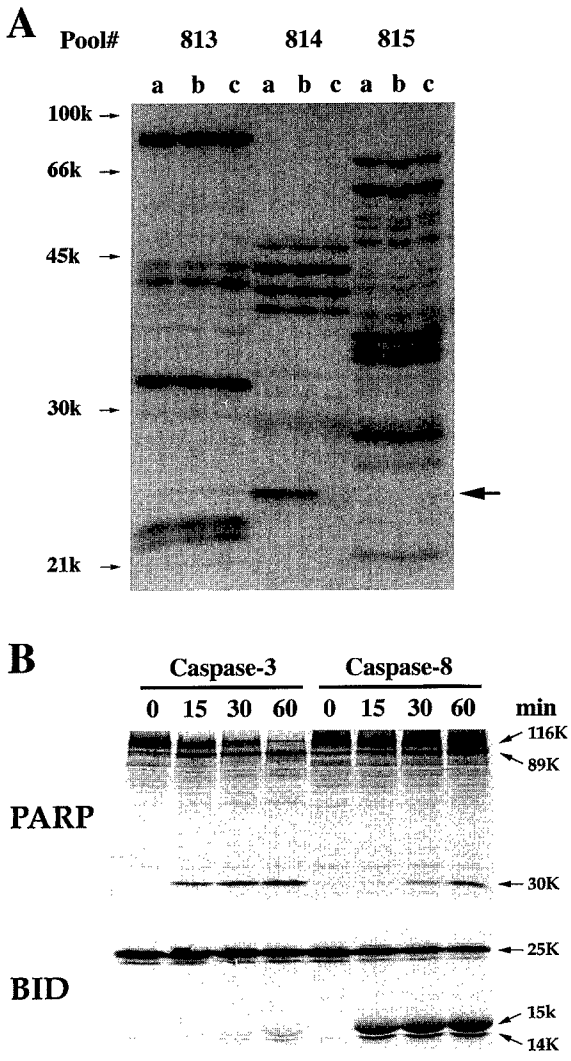

Figure 1. BID Is a Preferred Substrate of Caspase 8 In Vitro

(A) Primary screening of caspase substrates by small pool in vitro expression cloning. Different pools of ^{35}S-labeled proteins were incubated with bacterial lysates containing either no caspase (a), Casp2 (b), or Casp8 (c) for 2 hr at 37°C. The reactions were terminated and analyzed by 12% SDS-PAGE. An arrow points to a band, later identified as murine BID, that disappeared in the presence of Casp8.

(B) BID is a better substrate of Casp8 than of Casp3. ^{35}S-labeled N-terminal T7-tagged BID was incubated with either Casp3 or Casp8 for indicated time periods, and the cleavage products were analyzed by 15% SDS-PAGE.

BID Is Cleaved In Vivo during Fas- and TNFα-Induced Apoptosis

To examine the cleavage of BID in vivo, we generated a polyclonal antibody against human BID protein. Using this antibody for Western blots, we found that when Jurkat cells were induced to undergo apoptosis by anti-Fas antibody, BID was initially cleaved to a 15 kDa fragment and further to a 13 kDa fragment. The cleavage event occurred in the early stage of apoptosis and was comparable to the time courses of Casp7, -8 activation and PARP cleavage in Jurkat cells (Figure 2A). To rule out the possibility that the 15 kDa and 13 kDa BID fragments are newly synthesized novel protein products recognized by the BID antibody, we induced Jurkat cells to undergo apoptosis in the presence of cycloheximide (CHX), an inhibitor of protein synthesis, and anti-Fas antibody. The cleavage patterns of BID, Casp7, −8, and PARP were examined by immunoblotting. We found that the appearance of the BID fragments was not altered by the presence of CHX (data not shown). Thus, the 15 kDa and 13 kDa BID fragments are likely to be the cleavage products of full-length BID induced by apoptosis. The amount of the 15 kDa peptide was constant during the time course of apoptosis, possibly due to its rapid conversion to the 13 kDa peptide and subsequent degradation. The cleavage of BID in Fas-induced apoptosis was inhibitable by 100 μM of zVAD-fmk, a peptide inhibitor of caspases (Figure 2B). To confirm the cleavage of BID in vivo and to determine the approximate site of cleavage, we transiently transfected C-terminal Flag-tagged murine BID into HeLa cells, which were then treated by TNFα and CHX to induce the activation of Casp8 and apoptosis. A Western blot of the cell lysate was blotted by anti-FLAG antibody (Figure 2C). A 16 kDa Flag-tagged peptide was present in the apoptotic lysate and absent in the control lysate, confirming our in vivo cleavage data and suggesting that the cleavage site of BID is in the N-terminal portion of the protein.

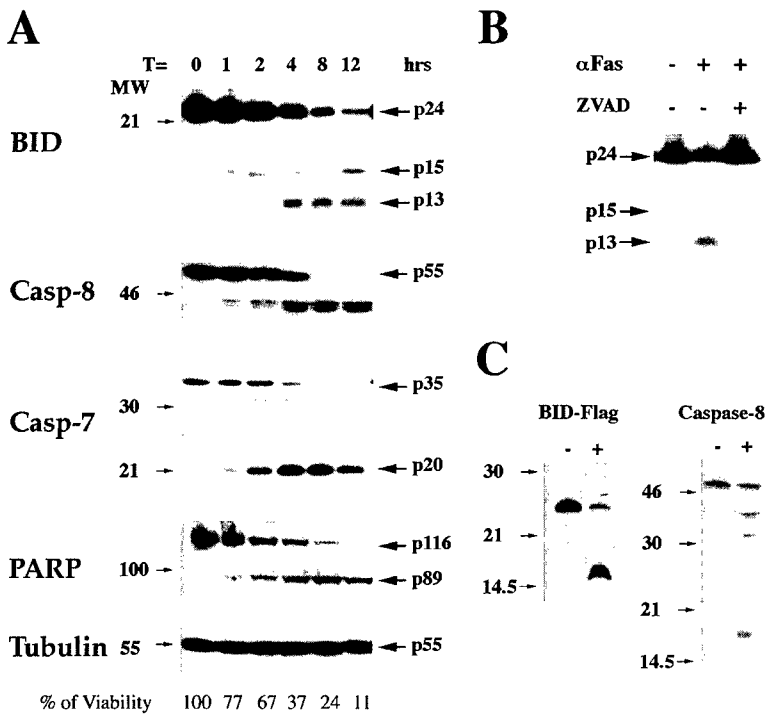

Figure 2. BID Is Cleaved In Vivo during Fas- and TNFα-Induced Apoptosis

(A) Time course of BID cleavage in Fas-induced apoptosis of Jurkat cells. The cell viability was determined by MTT assay and shown at the bottom of the figure.

(B) BID cleavage was inhibited with zVAD-fmk. Jurkat cells were preincubated with 100 μM of zVAD-fmk for 30 min and then incubated with anti-Fas antibody for 5 hr. Total cell lysates were prepared and blotted with anti-BID antibody. Arrows point to the full-length BID (p24) and two cleavage products, p15 and p13.

(C) C-terminal Flag-tagged BID was cleaved in TNFα-induced apoptosis of HeLa cells. Twenty-four hours after transient transfection of BID-Flag, HeLa cells were treated with either 1 μg/ml CHX alone (−) or 10 ng/ml TNFα and 1 μg/ml CHX (+) for 4 hr. Total cell lysates were subjected to Western blotting using either anti-Flag or anti-Casp8 antibodies. The molecular weight standard is shown on the left. A 16 kDa fragment is present specifically in the apoptotic HeLa cells transfected with BID-flag.

Determination of Cleavage Sites of BID

Two potential caspase cleavage sites reside in the N-terminal portion of murine BID: ^{56}Leu-Gln-Thr-Asp-Gly^{60} (LQTDG) and ^{72}Ile-Glu-Pro-Asp-Ser^{76} (IEPDS) (the corresponding sequences for human BID are ^{57}LQTDG^{61} and ^{72}IEADS^{76}). They match perfectly with the preferred cleavage sites for Casp8 and granzyme B, respectively, as determined by combinatorial peptide library screening (Thornberry et al., 1997). To confirm that they are indeed the cleavage sites for Casp8 and granzyme B, we mutated the two Asp residues to Glu either individually or both (namely mutant D59E, D75E, and DM). As shown in Figure 3A, N-terminal T7-tagged wild-type BID was completely cleaved by Casp1, -8, and granzyme B, and partially cleaved by Casp2 and −3. D59E BID mutant was only cleaved by granzyme B, not by caspases, while D75E BID mutant was cleaved efficiently by caspases, but not by granzyme B, suggesting that D75 is the cleavage site for granzyme B while D59 is the caspase cleavage site. As expected, the double mutant BID (DM BID) was cleaved by neither the caspases nor granzyme B. Two fragments of BID, a 15 kDa and a 14 kDa, were generated by caspase cleavage. The 14 kDa peptide was shifted to 13 kDa when a wild-type BID without N-terminal tag was cleaved by Casp8 (data not shown), suggesting that the 15 kDa peptide is the C-terminal part of BID and the 14 kDa peptide is the N-terminal portion with an anomalous mobility in SDS-PAGE. As an additional proof, the cleavage of BID by granzyme B generated a smaller C-terminal fragment and a larger N-terminal fragment that overlapped each other on SDS-PAGE (Figure 3A).

The Proapoptotic Activity of BID Strongly Depends upon Its Cleavage

BID was previously identified as a death agonist (Wang et al., 1996). Thus, it is interesting to examine whether its proapoptotic activity is enhanced by its cleavage. We cotransfected a *LacZ* construct with either wild-type BID or its cleavage-defective mutants into HeLa cells and then treated the cells with TNFα and CHX for 4 hr. The percentages of cell death expressing BID was determined by X-Gal staining. While 4 hr treatment of TNFα and CHX induced 54% of *LacZ*-transfected cells to die (*LacZ*-transfected control cells without treatment showed 3.8% of cell death, and WT BID–transfected cells without treatment showed 9.3% of cell death), the same TNFα and CHX treatment induced 91.5% of WT and 92.2% of D75E BID–transfected cells to die, respectively. Thus, the expression of wild-type and D75E BID increased TNFα-induced cell death by 69.4% and 69.5%, respectively, as shown in Figure 3B. In contrast, transfection of D59E and DM mutant BID had insignificant effects on TNFα-induced HeLa cell death (12.5% and 5.9%, respectively). The expression of BID and its mutants in transfected HeLa cells after TNFα treatment was also examined. Wild-type and D75E BID were cleaved into a 16 kDa fragment, but D59E and DM BID were not (Figure 3C). Thus, the proapoptotic activity of BID is strongly dependent upon its cleavage by Casp8 at D59.

The Cleaved BID Is a Potent Apoptosis-Inducing Agent

Most of the death agonists in the Bcl2 family contain a BH3 domain that is essential for their Bcl2 binding and proapoptotic activity (Chittenden et al., 1995; Wang et al., 1996; Kelekar et al., 1997) and capable of inducing caspase activation in a cell-free *Xenopus* oocyte system (Cosulich et al., 1997). It is possible that once BID is cleaved, the truncated portion containing the BH3 domain becomes lethal to cells. To investigate this possibility, we transiently transfected the C-terminal portion of BID (residue 60–195) (tBID) into Rat-1 fibroblast cells.

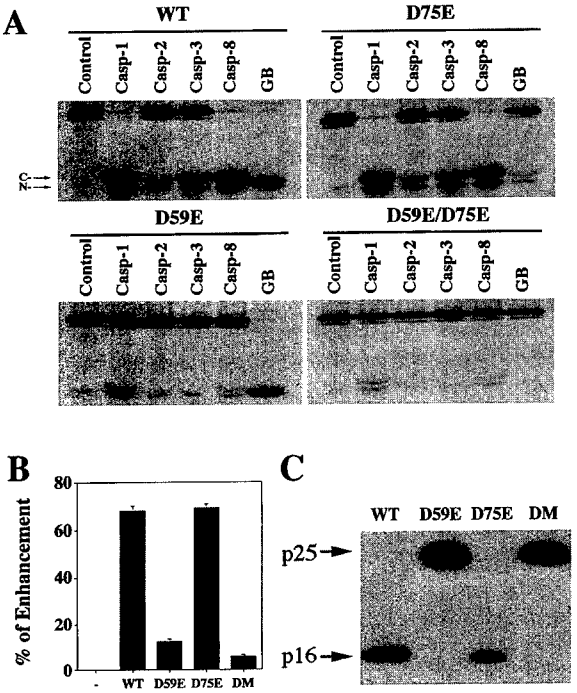

Figure 3. Proapoptotic Activity of BID Strongly Depends upon Its Cleavage

(A) Determination of cleavage sites of BID. ^{35}S-labeled wild-type BID or its mutants were incubated with either caspases or granzyme B and analyzed by SDS-PAGE. BID was cleaved by caspases into two fragments: the larger one (15 kDa) was the C-terminal fragment, and the smaller one (14 kDa) was the N-terminal fragment. The cleavage products of granzyme B overlapped each other.

(B) Wild-type BID and D75E mutant promoted TNFα-induced apoptosis of HeLa cells, while caspase cleavage–defective mutants (D59E and DM) did not. HeLa cells were transfected with either the expression constructs of Bid or its mutants with *LacZ* construct overnight and treated with 10 ng/ml TNFα and 1 μg/ml CHX for 4 hr. After fixation, X-Gal staining was performed, and the percentage of cell death was scored by cell morphology of blue cells (flat, well-attached versus round blue cells) as before (Miura et al., 1993).

(C) Cleavage of wild-type BID and its mutants in vivo. HeLa cells were transfected with the expression constructs of Bid or its mutants overnight and then treated with TNFα and CHX for 4 hr. The cell lysates were blotted with anti-Flag antibody. Arrows point to the full-length Flag-tagged BID (p25) and its cleavage product, p16.

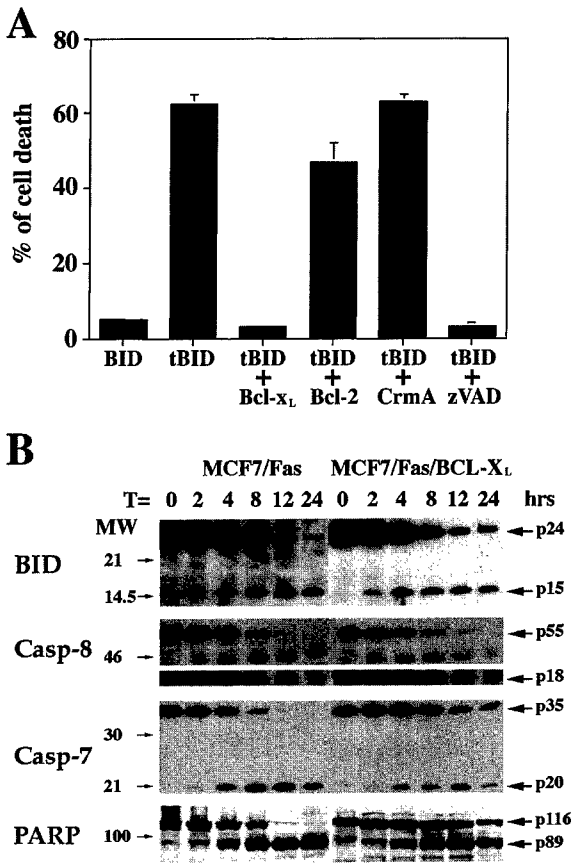

Figure 4. BID Acts Downstream of Casp8 and Upstream of Bclx$_L$ in Fas-Induced Apoptosis

(A) tBID-induced apoptosis of Rat-1 cells. Rat-1 cells seeded in 6-well plate were transfected with either 1 μg pcDNA-Bid or 0.25 μg pcDNA-tBid along with 1 μg *LacZ* construct. For different cell death inhibitors, 0.25 μg tBID was cotransfected with either 1 μg Bclx$_L$, 1 μg Bcl2, or 1 μg CrmA-expressing constructs, along with 1 μg *LacZ* construct. zVAD- fmk (100 μM) was added half an hour before transfection of tBid was performed. After 8 hr transfection, cells were fixed and X-Gal stained, and cell death percentage was scored by cell morphology of blue cells.

(B) Time course of BID cleavage in vivo. MCF7/Fas and MCF7/Fas/Bclx$_L$ cells were incubated with anti-Fas monoclonal antibody 7C11 (1:500) in the presence of 1 μg/ml CHX for different periods of time as indicated. Total cell lysates were then subjected to Western blotting analysis using antibodies against BID, Casp8, Casp7, and PARP. Arrows point to p24 (full-length BID), p15 (cleaved BID), p55 (full-length Casp8), p18 (cleaved Casp8), p35 (full-length Casp7), p20 (cleaved Casp7), p116 (full-length PARP), and p89 (cleaved PARP).

As shown in Figure 4A, full-length BID could not induce apoptosis, while tBID induced apoptosis very rapidly and efficiently. tBID-induced cell death was inhibited completely by Bclx$_L$ and zVAD-fmk, partially by Bcl2, but not at all by CrmA. This result suggests that the N terminus of BID has an inhibitory effect to its proapoptotic activity, and its removal by caspase cleavage yields tBID that is an effective inducer of downstream apoptotic events. The apoptosis-inducing activity of tBID is completely inhibited by Bclx$_L$, suggesting that BID may function upstream of Bclx$_L$/Bcl2. As CrmA can inhibit Casp1 and Casp8, but not other caspases (Zhou et al., 1997), the failure of CrmA to inhibit tBID-induced apoptosis is consistent with the hypothesis that BID acts downstream of Casp8.

BID Acts Downstream of Caspase 8 and Upstream of Bclx$_L$ in Fas-Induced Apoptosis

To examine whether BID is a specific proximal substrate of Casp8 and whether it operates upstream of Bclx$_L$/Bcl2, we used MCF7/Fas and its Bclx$_L$ stable cell lines. It has been shown that in MCF7 cells, Bclx$_L$ can prevent Fas- and TNFα-induced cell death and inhibit downstream caspase activation even though Casp8 is activated (Medema et al., 1998; Srinivasan et al., 1998). As shown in Figure 4B, the cleavage profile of BID correlated perfectly with the activation of Casp8, both of

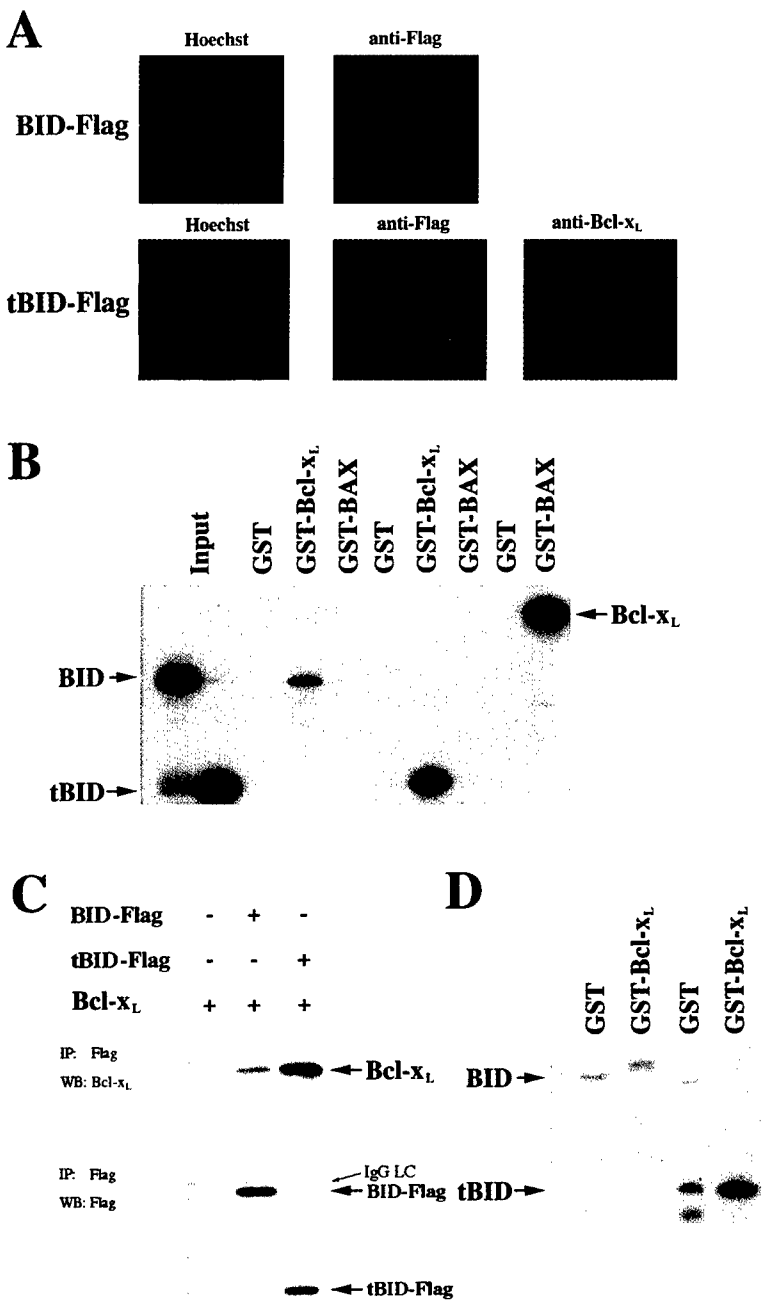

Figure 5. Truncated BID Has a Stronger Affinity for Bclx$_L$ than Its Precursor

(A) tBID was colocalized with Bclx$_L$. Constructs expressing BID-Flag or tBID-Flag fusion proteins were transiently transfected into HeLa/Bclx$_L$ stable cells. Immunohistochemistry was performed using anti-Flag antibody M2 and anti-Bclx$_L$ antibody.

(B) In vitro interactions between BID and Bclx$_L$ or Bax. ^{35}S-labeled BID or its cleaved form was incubated with either GST-Bclx$_L$ or GST-Bax bound to glutathione-agarose beads. After 3 hr incubation and three washes, the bound BID or tBID was analyzed by SDS-PAGE and autoradiography.

(C) In vivo interactions between BID and Bclx$_L$. Constructs expressing BID-Flag or tBID-Flag were cotransfected with Bclx$_L$ construct into HEK 293T cells. BID-Flag or tBID-Flag was immunoprecipitated by anti-Flag M2 affinity gel in the presence of 0.25% nonionic detergent IGEPAL CA-630 and Western blotted using anti-Bclx$_L$ antibody and M2 anti-Flag antibody, respectively.

(D) In vitro interaction between BID and Bclx$_L$ in the absence of nonionic detergent. ^{35}S-labeled BID or tBID was incubated with GST-Bclx$_L$ in a binding buffer without any nonionic detergent, and the bound BID or tBID was subjected to SDS-PAGE and autoradiography.

which were not altered by expression of Bclx$_L$. In contrast, the activation of Casp7 and the cleavage of PARP were delayed and partially inhibited by overexpression of Bclx$_L$. This result strongly supports our hypothesis that BID is a specific proximal substrate of Casp8 during Fas-induced apoptosis that functions upstream of Bclx$_L$.

Truncated BID Has a Stronger Affinity for Bclx$_L$ than the Full-Length BID

How does tBID induce apoptosis? It was proposed that BID, which localizes in cytoplasmic as well as in membrane fractions, acts as a ligand to Bcl2/Bclx$_L$ and Bax (Wang et al., 1996). We examined whether tBID behaves the same as its precursor. When tBID was overexpressed in HeLa/Bclx$_L$ stable cells, tBID colocalized with Bclx$_L$ (Figure 5A), suggesting that BID is translocated from cytoplasm to the membrane compartments when cleaved by Casp8. In contrast, the full-length BID was evenly distributed in every cellular compartment (Figure 5A). As BID does not have a membrane anchorage domain, one possible mechanism of translocation is that tBID has a stronger affinity to Bclx$_L$ than its precursor. To test this hypothesis, we examined the interaction between tBID and Bclx$_L$ in vitro and in vivo. We incubated ^{35}S-labeled BID or tBID with GST-Bclx$_L$ in vitro in the presence of 0.25% nonionic detergent IGEPAL CA-630,

and the amount of bound BID or tBID was analyzed by SDS-PAGE. As estimated by intensities of the corresponding bands, tBID has approximately 10-fold higher affinity toward GST-Bclx$_L$ fusion protein compared to its full-length precursor (Figure 5B), while the interaction between tBID and GST-Bax was undetectable. To examine the interaction of BID with Bclx$_L$ in vivo, we cotransfected the C-terminal Flag-tagged BID or its truncated form with Bclx$_L$ into HEK 293T cells and immunoprecipitated with anti-Flag M2 affinity gel in the presence of 0.25% nonionic detergent IGEPAL CA-630. The expression level of tBID was much lower than that of its precursor (data not shown). As shown in Figure 5C, much more Bclx$_L$ was coimmunoprecipitated with tBID than with full-length BID, and the difference was estimated around 20-fold by phosphoimager. It was reported that the presence of detergent in coimmunoprecipitation experiments affects the conformation of Bax and its interaction with Bcl2/Bclx$_L$ (Hsu and Youle, 1997), so we examined the interaction between BID and Bclx$_L$ in the absence of detergent. The interaction between the full-length BID and GST-Bclx$_L$ in the absence of detergent was not significantly different from the background, while the tBID C-terminal fragment, but not the N-terminal fragment, still bound effectively to Bclx$_L$ (Figure 5D). Thus, our in vivo and in vitro data indicate that the N-terminal domain of BID may have an inhibitory function, and the removal of the N-terminal domain exposes BID's BH3 domain to allow efficient interactions with other proteins.

Truncated BID Induces Mitochondrial Damage, Cell Shrinkage, and Nuclear Condensation

Mitochondrial damage and release of cytochrome c have been identified as key events in mediating activation of downstream caspases in apoptosis (Liu et al., 1996; Shimizu et al., 1996; Susin et al., 1996). Occurrence of these events is prevented by overexpression of Bcl2/Bclx$_L$ (Kluck et al., 1997; Vander Heiden et al., 1997; Yang et al., 1997). We postulated that tBID may be able to mediate mitochondrial damage that is inhibitable by Bclx$_L$. To illustrate the downstream events resulting from the cleavage of BID, we used an ecdysone-inducible system in which the tBID-GFP fusion gene was placed under the control of an ecdysone-inducible promoter. After transient transfection of tBID-GFP and transactivator pVgRXR overnight, the expression of tBID-GFP was induced by addition of 1 μM of muristerone A, an ecdysone analog, and examined by appearance of green fluorescence. Green fluorescence of tBID-GFP could be detected as early as 2 hr after induction (data not shown). Mitochondrial integrity was examined by fluorescent dye mitotracker, whose uptake depends on mitochondrial membrane potential, immunostaining of cytochrome c, which resides between inner and outer mitochondrial membranes, and cytochrome c oxidase subunit VIc (COX VIc), which resides within the inner mitochondrial membrane. The change of nuclear morphology was monitored by Hoechst dye staining. In the early stage of tBID-induced apoptosis, when nuclear morphology was largely normal, the signals of mitotracker, immunostaining of cytochrome c, and COX VIc began to fade in the periphery of the cells and became clustered around nuclei forming a ring (data not shown). As the apoptotic process proceeded, cells shrank and nuclei began to condense and fragment, and both signals of mitotracker and cytochrome c immunostaining became diffused, while immunostaining of COX VIc became intensified around shrunk nuclei (Figure 6A). This result suggests that tBID induces the clustering of mitochondria, release of cytochrome c, loss of mitochondrial membrane potential, cell shrinkage, and nuclear condensation. Green fluorescence of tBID-GFP exactly overlapped with COX VIc immunostaining in the early and late stages, further suggesting that tBID is targeted to the mitochondria.

Bclx$_L$ and Caspase Inhibitors Inhibit Distinct Steps in Apoptosis Induced by Truncated BID

To elucidate the mechanism of tBID-induced apoptosis, we examined the effects of various cell death inhibitors, such as CrmA, p35, zVAD-fmk, Casp9 (C287A) dominant negative mutant (DN), and Bclx$_L$, on tBID-induced mitochondrial damage, cell shrinkage, and nuclear condensation. Ninety-eight percent of MCF7/Fas cells underwent cell shrinkage and nuclear condensation and fragmentation at 4 hr after induction of tBID-GFP (Figures 6A and 6B). Among caspase inhibitors, CrmA had no effect, and p35 had a modest effect (32% inhibition), while zVAD-fmk inhibited most of tBID-induced cell shrinkage and nuclear condensation (90% inhibition) (Figures 6B and 6C), indicating that the caspase activity is required for tBID-induced cell shrinkage and nuclear condensation. Casp9 DN mutant also inhibited tBID-induced cell shrinkage and nuclear condensation, but was less effective than zVAD-fmk (71% inhibition) (Figure 6B), suggesting that BID acts upstream of Casp9/cytochrome c/Apaf1 pathway. Thirty hours after induction, most of the cells remained normal in the presence of zVAD-fmk (85%), while only 30% of nuclei were normal in the presence of Casp9 DN mutant (data not shown), indicating that Casp9 DN mutant can only delay, not block, the apoptotic process induced by tBID. Compared to other inhibitors, Bclx$_L$, which completely inhibited tBID-induced cell shrinkage and nuclear condensation, was the most effective antagonist of tBID's function (Figures 6B and 6D).

Although zVAD-fmk, Casp9 DN, and Bclx$_L$ have comparable effects on tBID-induced cell shrinkage and nuclear condensation, they had very different effects on tBID-induced mitochondrial damage. As shown in Figure 6D, the distribution of mitotracker, cytochrome c, and COX VIc in tBID/Bclx$_L$–expressing cells was the same as that in normal cells where green fluorescence of tBID-GFP overlapped with mitotracker signals and immunostaining of cytochrome c and COX VIc. In contrast, in the presence of zVAD-fmk, the signal of mitotracker disappeared from the peripheral region of cytoplasm and became aggregated around the nuclei, while immunostaining of cytochrome c completely disappeared (Figure 6C), suggesting that zVAD-fmk inhibits the loss of mitochondrial inner membrane potential but not the release of cytochrome c induced by tBID. The Casp9 DN mutant has a similar but less effective inhibitory activity (data not shown). As COX is an enzyme

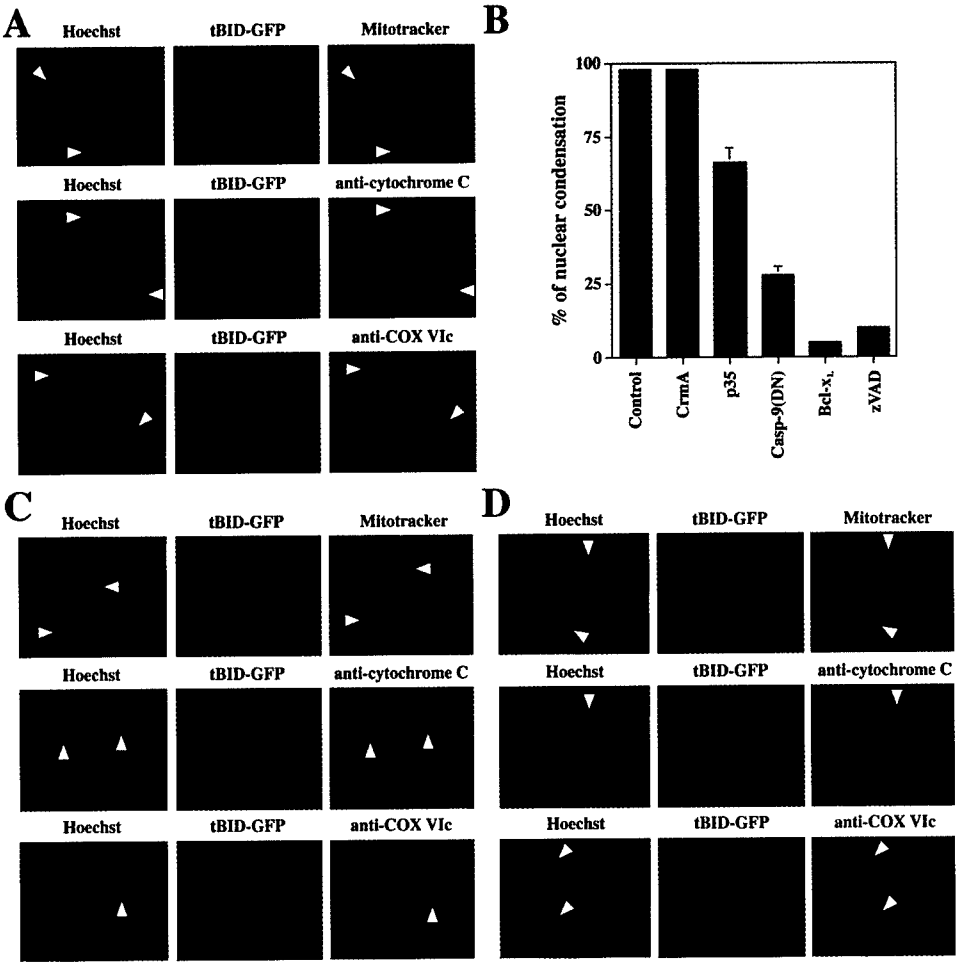

Figure 6. Differential Effects of $Bclx_L$ and zVAD-fmk on Truncated BID–Induced Apoptosis

(A) tBID-induced mitochondrial depolarization and the release of cytochrome c. MCF7/Fas cells were transfected with pIND-tBID-GFP and pVgRxR overnight and induced with muristerone A for 4 hr. For mitotracker staining, 300 nM Mitotracker CMTMRos was added into medium and then cells were fixed. For immunohistochemistry, cells were then fixed and immunostained with either anti-cytochrome c antibody or anti-COX VIc antibody. Arrows indicate the cells expressing tBID-GFP fusion protein.

(B) Effects of different cell death inhibitors on tBID-induced nuclear condensation. pIND-tBID-GFP and pVgRxR were transfected into MCF7/Fas or in combinations with different cell death inhibitors: CrmA, p35, Casp9 DN mutant, and $Bclx_L$. After overnight transfection, 1 μM of muristerone A was added into medium (for zVAD-fmk, cells were incubated with 100 μM of zVAD-fmk for half an hour prior to the addition of muristerone A). After 4 hr induction, cells were fixed and washed with PBS and then incubated with 1 ng/ml of Hoechst dye. Percentage of nuclear condensation was scored by nuclear morphology.

(C) zVAD-fmk–inhibited tBID-induced loss of mitochondrial membrane potential, indicated by the ability of mitochondria to uptake mitotracker, cell shrinkage, and nuclear condensation, but not mitochondrial clustering and cytochrome c release. Cells were incubated with 100 μM of zVAD-fmk for half an hour prior to addition of muristerone A. Similar experiments described in (B) were performed. Arrows indicate the cells expressing tBID-GFP fusion protein.

(D) $Bclx_L$ completely inhibited all apoptotic morphological changes induced by tBID. $Bclx_L$ construct was cotransfected into MCF7/Fas cells along with pIND-tBID-GFP and pVgRxR. After overnight transfection, similar experiments described in (B) were performed. Arrows indicate the cells expressing tBID-GFP fusion protein.

localized in the inner membrane of mitochondria, immunostaining of COX VIc is an indication of mitochondrial distribution. In contrast to the disappearance of cytochrome c immunostaining in the presence of zVAD-fmk, the signal of COX VIc immunostaining remained largely clustered around nuclei and overlapped with the tBID-GFP signal (Figure 6C). Taken together, these results suggest that tBID induces the redistribution of mitochondria and the release of cytochrome c in a caspase-independent process but does not cause a complete disruption of mitochondrial inner membrane in the presence of caspase inhibitors.

Truncated BID Induces the Release of Cytochrome c from Purified Mitochondria In Vitro

To examine the mechanism by which BID mediates mitochondrial damage, we evaluated its ability to induce cytochrome c release from partially purified mitochondria in a cell-free system. Partially purifed mitochondria were incubated with purified full-length BID or its truncated form, and the release of cytochrome c was examined. As shown in Figure 7, both full-length and tBID were able to induce the release of cytochrome c from mitochondria, but tBID was much more efficient than

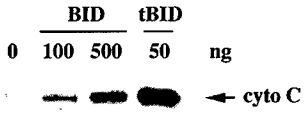

Figure 7. Truncated BID Induced the Release of Cytochrome c from Partially Purified Mitochondria In Vitro

Purified recombinant BID or tBID were incubated with partially purified mitochondria from mouse liver, and the released cytochrome c was examined by immunoblotting.

full-length BID. This result is consistent with our in vivo observation that tBID is more potent in its proapoptotic activity than its precursor.

Discussion

A number of BH3-containing death agonists of the Bcl2 family have been recently identified. Among them, a group of so-called "BH3-only" death agonists, including Bik/Bbk, BID, Hrk/DP5, and newly identified Blk and Bim, seem to be more potent in their apoptosis-inducing activity than other death agonists in the family that contains additional BH1 and BH2 domains such as Bad. Identification of *C. elegans egl-1* as a general component of programmed cell death machinery indicates that BH3-containing death agonists are important regulators in apoptosis (Conradt and Horvitz, 1998). The BH3 domain is the only homologous region shared by these BH3-only death agonists, indicating that they may use a common BH3 domain-mediated mechanism to induce apoptosis, although the regulation of their activities may be different from each other. BID differs from other BH3-only molecules by two characteristics: the absence of a C-terminal hydrophobic membrane anchor, and the presence of two perfect cleavage sites for Casp8 and granzyme B, respectively, which are not found in other BH3-only molecules. Although overexpression of full-length BID can induce apoptosis in certain cells (data not shown; Wang et al., 1996), its truncated form is much more potent, indicating that caspase cleavage is one of the mechanisms to regulate its proapoptotic activity. It was recently reported that death antagonists of the Bcl2 family, such as CED-9, Bcl2, and $Bclx_L$, can be cleaved by caspases (Cheng et al., 1997; Xue and Horvitz, 1997; Clem et al., 1998), indicating that caspase cleavage of Bcl2 family members is evolutionarily conserved and diversified.

We presented the evidence of BID translocation from cytosol to mitochondria during propagation of a death signal. Such translocation during apoptosis has been observed for two additional members of the Bcl2 family, Bax and BAD. It was reported that Bax moves from cytosol to mitochondria during apoptosis, although the regulatory mechanism of Bax translocation is unclear (Wolter et al., 1997). BAD exhibits a similar behavior when FL5.12 cells are starved for IL-3 and the translocation is regulated by protein phosphorylation (Zha et al., 1996). Translocation from cytosol to mitochondria may be an important activating mechanism for the proapoptotic members of the Bcl2 family and the propagation of apoptotic signals intracellularly. Caspase cleavage–induced BID translocation represents a novel mechanism to release the proapoptotic potential of BID, perhaps by removing the inhibitory N-terminal domain, exposing BH3 domain and allowing tBID to interact with its receptor on the mitochondria.

Availability of different cell death inhibitors allowed us to map accurately the position of BID in the Fas signaling pathway and to study the downstream events after BID cleavage. The first detectable morphological change induced by tBID is the clustering of mitochondria around the nuclei at a stage when cytochrome c appears to remain largely within the mitochondria and mitotracker uptake is normal. Such movement of mitochondria has not been detected previously during the Fas-induced apoptosis, which may be because of two reasons. First, Fas-induced apoptosis can activate multiple apoptotic downstream events that occur very fast, and thus it may be difficult to capture such an intermediate step. Second, caspase inhibitors such as CrmA, p35, and zVAD-fmk are all effective inhibitors of Casp8, and thus they inhibit the activation of Casp8 itself and prevent the activation of downstream events altogether. Truncated BID allows us to bypass the requirement of Casp8 to dissect the downstream events of the Fas pathway. Why do mitochondria appear to be clustering around nuclei in the early stage of tBID-induced apoptosis? One possible explanation is that mitochondria are damaged sequentially, with mitochondria closest to the cytoplasmic membrane being damaged first. Alternatively, tBID may be able to induce not only mitochondrial leakage but also their detachment from cytoskeletal structure, resulting in their collapsing around nuclei. More experiments will be done to distinguish these two possibilities.

The second detectable morphological change in tBID-induced apoptosis appears to be the release of cytochrome c while mitotracker uptake is still normal. In the presence of zVAD-fmk, we can see rings of mitochondria that are mitotracker-positive and COX VIc–positive, while cytochrome c immunostaining has disappeared. Since cytochrome c resides between the inner and outer mitochondrial space, mitotracker uptake depends upon mitochondrial membrane potential, and COX VIc resides in the inner mitochondrial membrane, our results suggest that tBID may be able to cause disruption of the outer mitochondrial membrane directly, while the disruption of inner mitochondrial membrane needs the help from caspase. Our results are consistent with the observation of Vander Heiden et al. (1997), who have suggested that in apoptosis the disruption of outer mitochondrial membrane occurs before the loss of mitochondrial membrane potential, which is mainly an indication of the inner mitochondrial membrane integrity. Our results are also consistent with the observation of Bossy-Wetzel et al. (1998), who showed that the loss of mitochondrial membrane potential, but not cytochrome c release of CEM and HeLa cells induced by UVB irradiation or staurosporine treatment, can be inhibited by zVAD-fmk. We suggest that BID or related BH3 domain–containing proteins may be involved in inducing mitochondrial damage in apoptosis induced by other stimuli as well, although the mechanism of activation may be different.

Although caspase inhibitors such as Casp9 DN, p35, and zVAD-fmk are unable to inhibit the early mitochondrial damages induced by tBID, they can inhibit the loss of mitochondrial membrane potential, cell shrinkage, and nuclear condensation induced by tBID with different effectiveness. While CrmA does not inhibit tBID-induced cell death, and p35 has a modest effect, zVAD-fmk is very effective in inhibiting tBID-induced nuclear condensation and in halting apoptotic process at an early stage when mitochondria cluster around normal-looking nuclei. The inhibitory activity of Casp9 DN mutant is similar to that of zVAD-fmk but less effective. Although this spectrum of inhibitor profile does not allow us to identify positively the critical caspase(s) involved in this process, it does suggest, however, that the release of cytochrome c may not be the only critical event downstream from the mitochondrial damage induced by tBID, since Casp9 DN is only partially effective in inhibition of tBID-induced cell death. This conclusion is also supported by the fact that tBID induces apoptosis of MCF7/Fas cells effectively, while microinjection of cytochrome c to MCF7/Fas cells does not induce apoptosis (Li et al., 1997a). Alternatively, tBID may activate downstream caspases by a cytochrome c–independent pathway in which tBID simply competes $Bclx_L$ from $Bclx_L$/Apaf1/caspase complex and activates downstream caspases. The observation that the Apaf1/Casp9/$Bclx_L$ complex exists (Hu et al., 1998; Pan et al., 1998) provides additional support for this model. These two mechanisms, however, are not mutually exclusive, and the mechanism by which tBID acts may be cell type–specific.

In contrast to caspase inhibitors, $Bclx_L$ can fully block the tBID's activity. Thus, the interaction of tBID with $Bclx_L$ must be the key to its ability to induce apoptosis. Kelakar et al. (1997) reported recently that wild-type BAD fails to induce apoptosis in response to growth factor withdrawal when cells are protected by a $Bclx_L$ mutant that does not bind to the BAD BH3 domain, suggesting that the interaction between the BH3 domain and Bcl2/$Bclx_L$ is critical for BH3 domain's proapoptotic activity. tBID may behave as an intracellular ligand for $Bclx_L$, which acts as the receptor in the Fas pathway. Unlike the conventional ligand–receptor interactions at cytoplasmic membrane, where such interactions usually result in the activation of the receptor, the interaction of tBID with $Bclx_L$ results in the inactivation of protective functions of $Bclx_L$ (or may we call it the activation of apoptotic-inducing functions of $Bclx_L$?). Alternatively, tBID may be capable of triggering apoptosis on its own, which may be Bcl2/$Bclx_L$–inhibitable, or Bcl2/$Bclx_L$ may simply act as a neutralizer of its death-inducing activity. These are interesting questions for future experiments. The dimeric interactions of antiapoptotic members of the Bcl2 family with proapoptotic members of the Bcl2 have been hypothesized to be an important mechanism of regulation (Oltvai and Korsmeyer, 1994). Recently, however, this view has been questioned mainly because of two works. First, Knudson and Korsmeyer (1997) reported that, in a genetic analysis, Bcl2 and Bax are able to act independently. Second, Hsu and Youle (1997) reported that the dimeric interaction of Bcl2 and Bax can only be detected in the presence of detergent, suggesting that detergent may induce specific conformational changes, exposing the interacting domain of Bcl2 and Bax and allowing such dimerization to occur. Interestingly, while we can detect the interaction of full-length BID with $Bclx_L$ in the presence of detergent, such interaction appears to be largely absent in the absence of detergent. In contrast, the interaction of tBID with $Bclx_L$ is still very strong in the absence of detergent. Our results indicate that the interaction of tBID with $Bclx_L$ is not induced by detergent. On the other hand, nonionic detergent appears to enhance the binding of full-length BID with $Bclx_L$, suggesting that detergent may be able to induce the conformational change of BID by removing the inhibition of N-terminal domain, a hypothesis that can be examined directly by further experimentation.

Experimental Procedures

Construction of Mouse Spleen cDNA Small Pool Library and In Vitro Expression Cloning

A mouse spleen cDNA library of 2×10^5 independent clones was constructed by using a Stratagene cDNA synthesis and cloning kit (Stratagene, La Jolla, CA), and cDNAs were inserted into EcoRI and XhoI sites of pCS2. Pools of cDNAs and in vitro translations were done as described by Lustig et al. (1997). The caspase cleavage assay was performed as described previously (Li et al., 1997b). The individual positive cDNA was identified using 96-well plates as described (Lustig et al., 1997), was sequenced, and compared with known sequences by searching the GenBank database.

Bacterial and Mammalian Expression Constructs of Murine and Human Bid and Generation of Anti-BID Antibody

The original clone of murine *Bid* obtained from the small pool library contained the full-length open reading frame of Bid. The standard molecular cloning methods and PCR were used to construct various mammalian expression vectors of murine Bid.

The full-length human BID gene was amplified by PCR from EST cDNA clone 52055 (Research Genetics, Inc., Huntsville, AL) and then cloned into the BamHI site of pGEX-2T. GST-BID fusion protein was purified by GST beads, GST was removed by thrombin digestion, and the purified BID protein was injected into rats to generate polyclonal antibody.

To establish an inducible expression system of tBid, tBid was inserted into BamHI site in frame with GFP (green fluorescence protein) in pEGFP-N1 vector (CLONTECH, Palo Atlo, CA), generating tBID-GFP fusion gene. The cassette of tBID-GFP was then cloned into EcoRI and NotI sites of pIND (Invitrogen, San Diego, CA).

Site-Directed Mutagenesis of the Cleavage Sites of Bid

Aspartic acid residues at positions 59 and 75 of Bid were mutated to glutamic acid individually or in combination, using QuickChange site-directed mutagenesis kit (Stratagene), following the supplier's instruction. Mutated sites were verified by DNA sequencing.

Tissue Culture Cells

Jurkat cells were cultured in RPMI 1640 supplemented with 10% fetal bovine serum (FBS), and HeLa and HEK 293T cells were cultured in DMEM containing 10% FBS. MCF7/Fas and MCF7/Fas/$Bclx_L$ stable cells were cultured in RPMI 1640 containing 10% FBS, 200 μg/ml G418, and 100 μg/ml hygromycin (Srinivasan et al., 1998).

Immunohistochemistry

For Mitotracker staining, Mitotracker CMTMRos (Molecular Probes Inc., Eugene, OR) was added to medium in a final concentration of 300 nM, and cells were further cultured for 30 min and fixed in 4% paraformadehyde for 15 min. Immunohistochemistry of cytochrome c and COX VIc was done according to Srinivasan et al. (1998), with minor modifications.

In Vitro and In Vivo Binding Assays

^{35}S-labeled BID or its cleaved form was incubated with 10 μg GST-$Bclx_L$ in 100 μl of the binding buffer (10 mM HEPES [pH 7.5], 150 mM KCl, 5 mM $MgCl_2$, 1 mM EDTA, and 0.25% IGEPAL CA-630) at

4°C for 3 hr with agitation. After brief centrifugation, beads were washed three times with 400 μl of binding buffer and resuspended in protein sample buffer. The samples were subjected to SDS-PAGE and autoradiography.

For in vivo binding assay, constructs expressing BID-Flag or tBID-Flag fusion protein were cotransfected with the construct expressing $Bclx_L$ into HEK 293T cells by a calcium-phosphate method. After 24 hr, cells were lysed in 1 ml of binding buffer, and total cell lysates were centrifuged at 10,000 × g for 15 min. M2 anti-Flag affinity gel (30 μl) was added into the supernatant, and the resulting mixture was incubated at 4°C for 3 hr with agitation. Following three washes, the beads were resuspended in appropriate amounts of protein sample buffer. The samples were subjected to Western blotting analysis.

Cell-Free Assay for the Release of Cytochrome c from Purified Mouse Liver Mitochondria

Mitochondria were purified as described by Shimizu et al. (1998). For in vitro assay, 5 μl of purified mitochondria was incubated with purified BID or tBID at 37°C for 1 hr. The reaction mixture was then centrifuged at 10,000 × g for 10 min, and the supernatant was subjected to SDS-PAGE and immunoblotting using anti-cytochrome c antibody.

Acknowledgments

We thank Dr. Marc Kirschner and the members of his laboratory for helpful advice on constructing and using the small pool expression library, which was critical for the success of this project. We thank Kevin Welch, Xun Clare Zhou, and members of the Yuan laboratory for a joint effort in preparing the small pool cDNA library, which was a lot of work. We thank Dr. Arnold Greenberg for providing granzyme B; Dr. Vishva Dixit for permission to use MCF7/Fas and MCF7/Fas/$Bclx_L$ cells; Dr. Emad Alnemri for Casp9 DN; Drs. Yoshihide Tsujimoto and Xiaodong Wang for protocols and advice on preparation of mitochondria; and Dr. Zhi-Jun Lu for GST-Bax. We also thank Xun Clare Zhou, Roberto Sanchez-Olea, Suyue Wang, Louise Bergeron, and Qiang Yu for their critical reading of the manuscript. This work was supported in part by a postdoctoral fellowship from National Institute of Aging (to H. L.), a grant from the Army's Breast Cancer Program (to J. Y.), and an American Heart Established Investigatorship (to J. Y.).

Received May 19, 1998; revised July 20, 1998.

References

Boldin, M.P., Goncharov, T.M., Goltsev, Y.V., and Wallach, D. (1996). Involvement of MACH, a novel MORT1/FADD-interacting protease, in Fas/APO-1- and TNF receptor-induced cell death. Cell *85*, 803–815.

Bossy-Wetzel, E., Newmeyer, D.D., and Green, D.R. (1998). Mitochondrial cytochrome C release in apoptosis occurs upstream of DEVD-specific caspase activation and independent of mitochondrial transmembrane depolarization. EMBO J. *17*, 37–49.

Cheng, E.H., Kirsch, D.G., Clem, R.J., Ravi, R., Kastan, M.B., Bedi, A., Ueno, K., and Hardwick, J.M. (1997). Conversion of Bcl-2 to a Bax-like death effector by caspases. Science *278*, 1966–1968.

Chittenden, T., Flemington, C., Houghton, A.B., Ebb, R.G., Gallo, G.J., Elangovan, B., Chinnadurai, G., and Lutz, R.J. (1995). A conserved domain in Bak, distinct from BH1 and BH2, mediates cell death and protein binding functions. EMBO J. *14*, 5589–5596.

Clem, R.J., Cheng, E.H., Karp, C.L., Kirsch, D.G., Ueno, K., Takahashi, A., Kastan, M.B., Griffin, D.E., Earnshaw, W.C., Veliuona, M.A., et al. (1998). Modulation of cell death by Bcl-x_L through caspase interaction. Proc. Natl. Acad. Sci. USA *95*, 554–559.

Conradt, B., and Horvitz, H.R. (1998). The *C. elegans* protein EGL-1 is required for programmed cell death and interacts with the Bcl-2-like protein CED-9. Cell *93*, 519–529.

Cosulich, S.C., Worrall, V., Hedge, P.J., Green, S., and Clarke, P.R. (1997). Regulation of apoptosis by BH3 domains in a cell-free system. Curr. Biol. *7*, 913–920.

Cryns, V., and Yuan, J. (1998). Proteases to die for. Genes Dev. *12*, 1551–1570.

Fernandes-Alnemri, T., Armstrong, R.C., Krebs, J., Srinivasula, S.M., Wang, L., Bullrich, F., Fritz, L.C., Trapani, J.A., Tomaselli, K.J., Litwack, G., et al. (1996). In vitro activation of CPP32 and Mch3 by Mch4, a novel human apoptotic cysteine protease containing two FADD-like domains. Proc. Natl. Acad. Sci. USA *93*, 7464–7469.

Hsu, Y.-T., and Youle, R.J. (1997). Nonionic detergents induces dimerization among members of the Bcl-2 family. J. Biol. Chem. *272*, 13829–13834.

Hu, Y., Benedict, M.A., Wu, D., Inohara, N., and Nunez, G. (1998). Bcl-x_L interacts with Apaf-1 and inhibits Apaf-1-dependent caspase-9 activation. Proc. Natl. Acad. Sci. USA *95*, 4386–4391.

Huang, D.C.S., Adams, J.M., and Cory, S. (1998). The conserved N-terminal BH4 domain of Bcl-2 homologues is essential for inhibition of apoptosis and interaction with CED-4. EMBO J. *17*, 1029–1039.

Kelekar, A., Chang, B.S., Harlan, J.E., and Thompson, C.B. (1997). Bad is a BH3 domain–containing protein that forms an inactivating dimer with Bcl-X_L. Mol. Cell. Biol. *17*, 7040–7046.

Kischkel, F.C., Hellbardt, S., Behrmann, I., Germer, M., Pawlita, M., Krammer, P.H., and Peter, M.E. (1995). Cytotoxicity-dependent APO-1 (Fas/CD95)-associated proteins form a death-inducing signaling complex (DISC) with the receptor. EMBO J. *14*, 5579–5588.

Kluck, R.M., Bossy-Wetzel, E., Green, D.R., and Newmeyer, D.D. (1997). The release of cytochrome c from mitochondria: a primary site for Bcl-2 regulation of apoptosis. Science *275*, 1132–1136.

Knudson, C.M., and Korsmeyer, S.J. (1997). Bcl-2 and Bax function independently to regulate cell death. Nat. Genet. *16*, 358–363.

Li, F., Srinivasan, A., Wang, Y., Armstrong, R.C., Tomaselli, K.J., and Fritz, L.C. (1997a). Cell-specific induction of apoptosis by microinjection of cytochrome c. Bcl-x_L has activity independent of cytochrome c release. J. Biol. Chem. *272*, 30299–30305.

Li, H., Bergeron, L., Cryns, V., Pasternack, M.S., Zhu, H., Shi, L., Greenberg, A., and Yuan, J. (1997b). Activation of caspase-2 in apoptosis. J. Biol. Chem. *272*, 21010–21017.

Li, P., Nijhawan, D., Brudihardjo, I., Srinivasula, S.M., Ahmad, M., Alnemri, E.S., and Wang, X. (1997c). Cytochrome C and dATP-dependent formation of Apaf-1/caspase-9 complex initiates an apoptotic protease cascade. Cell *91*, 479–489.

Liu, X., Kim, C.N., Yang, J., Jemmerson, R., and Wang, X. (1996). Induction of apoptotic program in cell free extracts: requirement for dATP and cytochrome C. Cell *86*, 147–157.

Lustig, K.D., Stukenberg, P.T., McGarry, T.J., King, R.W., Cryns, V.L., Mead, P.E., Zon, L.I., Yuan, J., and Kirschner, M.W. (1997). Small pool expression screening: identification of genes involved in cell cycle control, apoptosis, and early development. Methods Enzymol. *283*, 83–99.

Medema, J.P., Scaffidi, C., Krammer, P.H., and Peter, M.E. (1998). Bcl-x_L acts downstream of caspase-8 activation by the CD95 death-inducing signaling complex. J. Biol. Chem. *273*, 3388–3393.

Merry, D.E., and Korsmeyer, S.J. (1997). Bcl-2 gene family in the nervous system. Annu. Rev. Neurosci. *20*, 245–267.

Miura, M., Zhu, H., Rotello, R., Hartwieg, E.A., and Yuan, J. (1993). Induction of apoptosis in fibroblasts by IL-1β-converting enzyme, a mammalian homolog of the *C. elegans* cell death gene *ced-3*. Cell *75*, 653–660.

Muzio, M., Chinnaiyan, A.M., Kischkel, F.C., O'Rourke, K., Shevchenko, A., Ni, J., Scaffidi, C., Bretz, J.D., Zhang, M., Gentz, R., et al. (1996). FLICE, a novel FADD-homologous ICE/CED-3-like protease, is recruited to the CD95 (Fas/APO-1) death-inducing signaling complex. Cell *85*, 817–827.

Oltvai, Z.N., and Korsmeyer, S.J. (1994). Checkpoints of dueling dimers foil death wishes. Cell *79*, 189–192.

Pan, G., O'Rourke, K., and Dixit, V.M. (1998). Caspase-9, Bcl-x_L, and Apaf-1 form a ternary complex. J. Biol. Chem. *273*, 5916–5922.

Salvesen, G.S., and Dixit, V.M. (1997). Caspases: intracellular signaling by proteolysis. Cell *91*, 443–446.

Scaffidi, C., Fulda, S., Srinivasan, A., Friesen, C., Li, F., Tomaselli,

K.J., Debatin, K.M., Krammer, P.H., and Peter, M.E. (1998). Two CD95 (APO-1/Fas) signaling pathways. EMBO J. *17*, 1675–1687.

Shimizu, S., Eguchi, Y., Kamiike, W., Waguri, S., Uchiyama, Y., Matsuda, H., and Tsujimoto, Y. (1996). Bcl-2 blocks loss of mitochondrial membrane potential while ICE inhibitors act a different step during inhibition of death induced by respiratory chain inhibitors. Oncogene *13*, 21–29.

Shimizu, S., Eguchi, Y., Kamiike, W., Funahashi, Y., Mignon, A., Lacronique, V., Matsuda, H., Tsujimoto, Y. (1998). Bcl-2 prevents apoptotic mitochondrial dysfunction by regulating proton flux. Proc. Natl. Acad. Sci. USA *95*, 1455–1459.

Srinivasan, A., Li, F., Wong, A., Kodandapani, L., Smidt, R., Jr., Krebs, J.F., Fritz, L.C., Wu, J.C., and Tomaselli, K.J. (1998). Bcl-x_L functions downstream of caspase-8 to inhibit Fas- and tumor necrosis factor receptor 1-induced apoptosis of MCF7 breast carcinoma cells. J. Biol. Chem. *273*, 4523–4529.

Susin, S.A., Zamzami, N., Castedo, M., Hirsch, T., Marchetti, P., Macho, A., Daugas, E., Geuskens, M., and Kreomer, G. (1996). Bcl-2 inhibits the mitochondrial release of an apoptogenic protease. J. Exp. Med. *184*, 1331–1341.

Thornberry, N.A., Rano, T.A., Peterson, E.P., Rasper, D.M., Timkey, T., Garcia-Calvo, M., Houtzager, V.M., Nordstrom, P.A., Roy, S., Vaillancourt, J.P., et al. (1997). A combinatorial approach defines specificities of members of the caspase family and granzyme B. Functional relationships established for key mediators of apoptosis. J. Biol. Chem. *272*, 17907–17911.

Vander Heiden, M.G., Chandel, N.S., Williamson, E.K., Schmacker, P.T., and Thompson, C.B. (1997). Bcl-x_L regulates the membrane potential and volume homeostasis of mitochondria. Cell *91*, 627–637.

Wang, K., Yin, X.-M., Chao, D.T., Milliman, C.L., and Korsmeyer, S.J. (1996). BID: a novel BH3 domain-only death agonist. Genes Dev. *10*, 2859–2869.

Wolter, K.G., Hsu, Y., Smith, C.L., Nechushtan, A., Xi, X., and Youle, R.J. (1997). Movement of Bax from the cytosol to mitochondria during apoptosis. J. Cell. Biol. *139*, 1281–1292.

Xue, D., and Horvitz, H.R. (1997). *Caenorhabditis elegans* CED-9 protein is a bifunctional cell-death inhibitor. Nature *390*, 305–308.

Yang, E., Zha, J., Jockel, J., Boise, L.H., Thompson, C.B., and Korsmeyer, S.J. (1995). Bad, a heterodimeric partner for Bcl-xl and Bcl-2, displaces Bax and promotes cell death. Cell *80*, 285–291.

Yang, J., Liu, X., Bhalla, K., Kim, C.N., Ibrado, A.M., Cai, J., Peng, T.I., Jones, D.P., and Wang, X. (1997). Prevention of apoptosis by Bcl-2: release of cytochrome C from mitochondria blocked. Science *275*, 1129–1132.

Zha, J., Harada, H., Yang, E., Jockel, J., and Korsmeyer, S.J. (1996). Serine phosphorylation of death agonist BAD in response to survival factor results in binding to 14–3–3 not BCL-X_L. Cell *87*, 619–626.

Zhou, Q., Snipas, S., Orth, K., Muzio, M., Dixit, V.M., and Salvesen, G.S. (1997). Target protease specificity of the viral serpin CrmA. Analysis of five caspases. J. Biol. Chem. *272*, 7797–7800.

Zou, H., Henzel, W.J., Liu, X., Lutschg, A., and Wang, X. (1997). Apaf-1, a human protein homologous to *C. elegans* CED-4, participates in cytochrome c-dependent activation of caspase-3. Cell *90*, 405–413.

Cell, Vol. 96, 615–624, March 5, 1999, Copyright ©1999 by Cell Press

Solution Structure of BID, an Intracellular Amplifier of Apoptotic Signaling

James J. Chou,*† Honglin Li,‡
Guy S. Salvesen,§ Junying Yuan,‡
and Gerhard Wagner*†‖
*Committee on Higher Degrees in Biophysics
Harvard University
Cambridge, Massachusetts 02138
†Department of Biological Chemistry and Molecular Pharmacology
‡Department of Cell Biology
Harvard Medical School
Boston, Massachusetts 02115
§The Burnham Institute
San Diego, California 92037

Summary

We report the solution structure of BID, an intracellular cross-talk agent that can amplify FAS/TNF apoptotic signal through the mitochondria death pathway after Caspase 8 cleavage. BID contains eight α helices where two central hydrophobic helices are surrounded by six amphipathic ones. The fold resembles pore-forming bacterial toxins and shows similarity to BCL-X_L although sequence homology to BCL-X_L is limited to the 16-residue BH3 domain. Furthermore, we modeled a complex of BCL-X_L and BID by aligning the BID and BAK BH3 motifs in the known BCL-X_L–BAK BH3 complex. Additionally, we show that the overall structure of BID is preserved after cleavage by Caspase 8. We propose that BID has both BH3 domain–dependent and –independent modes of action in inducing mitochondrial damage.

Introduction

The intracellular FAS signal transduction pathway of apoptosis is initiated when Procaspase 8 is recruited to the death-induced signaling complex (DISC) through interaction with the adapter molecule FADD/MORT1 (Boldin et al., 1996; Muzio et al., 1996). The local aggregation of Procaspase 8 is sufficient to allow auto- or transprocessing to produce active Caspase 8 (reviewed by Green, 1998; Muzio et al., 1998; Yang et al., 1998), which can subsequently activate executioners such as Caspases 3, 6, and 7. An alternative amplification pathway leading to large-scale activation of downstream caspases is through mitochondrial damage. This pathway is initiated upon cytochrome c release from mitochondria. Cytochrome c, in the presence of dATP, triggers the activation of Caspase 9 through Apaf1/Caspase 9 complex formation (Li et al., 1997). For the mitochondria pathway, Caspase 9 is the central initiator that activates the downstream executioners such as Caspases 3, 6, and 7. Although activated Caspase 8 can lead directly to downstream caspase activation in certain cell types, mitochondria are the essential mediators in others (Scaffidi et al., 1998). In cell-free *Xenopus* egg extracts, the ability of small amounts of Caspase 8 to trigger activation of downstream caspases was dependent on the presence of mitochondria (Kuwana et al., 1998). In extracts devoid of mitochondria, high concentrations of Caspase 8 were required to activate downstream caspases. However, when mitochondria were present, the trigger of downstream caspase activation from low concentration of Caspase 8 was vastly amplified through cytochrome c release after mitochondrial damage.

While mitochondrial damage is the major amplification step in the apoptotic pathway, the mitochondrion is also the principal site of action for pro- and antiapoptotic members of the BCL2 superfamily. The BCL2 family of proteins shares amino acid sequence homology in one to four regions designated the BCL2 homology (BH) domains: BH1, BH2, BH3, and BH4 (reviewed by Kelekar and Thompson, 1998). The two well-known antiapoptotic members BCL2 and BCL-X_L are usually localized on the cytoplasmic face of the mitochondrial outer membrane. Overexpression of BCL2 or BCL-X_L blocks the release of cytochrome c and aborts the apoptotic response (Kluck et al., 1997; Yang et al., 1997). The survival function of BCL2 has also been implicated in its binding to the CED4-like portion of Apaf1 to thereby prevent the activation of Procaspase 9 (Hu et al., 1998; Pan et al., 1998). In addition, both BCL2 and BCL-X_L have been shown to form selective ion channels in lipid membranes (Minn et al., 1997), which may regulate the mitochondrial membrane potential and thus prevent cytochrome c release. The proapoptotic members of the BCL2 family include BAX, which contains multiple BH homology domains (BH1, BH2, and BH3), as well as a class of molecules sharing only the BH3 homology, such as BIK, BAD, BID, and EGL1 (reviewed by Adams and Cory, 1998). The BH3 domain of the proapoptotic members of the BCL2 superfamily has been shown to interact with antiapoptotic members of the family (see review by Kelekar and Thompson, 1998). Furthermore, the BH3 domains from proapoptotic, but not antiapoptotic, members of the BCL2 family can induce the release of cytochrome c from isolated mitochondria (Cosulich et al., 1997). These results suggest that the heterodimerization of pro- and antiapoptotic members of the BCL2 family may be critical for killing induced by BAX-like molecules. Recently, however, multiple lines of evidence suggest that proapoptotic functions of BAX-like molecules go beyond its ability to bind BCL2 or BCL-X_L through the BH3 domains. Genetic studies indicated that BCL2 and BAX function independently to regulate apoptosis in nonlymphoid cell lineages as well as lymphoid cell lineages other than thymocytes (Knudson and Korsmeyer, 1997). Mutagenesis of the BAX BH3 domain, which eliminated the ability of BAX to interact with BCL2 and BCL-X_L, did not perturb its ability to induce apoptosis (Wang et al., 1998). These results suggest that BAX-like molecules have an important mechanism of killing that is independent of the BH3

‖To whom correspondence should be addressed (e-mail: wagner@wagner.med.harvard.edu).

domain, although the structural basis of this mechanism is unclear.

BID is a proapoptotic member of the BCL2 family that shares only the BH3 domain homology with other members of the family in its amino acid sequence. It has recently been established as an intracellular messenger connecting the FAS receptor and the death-inducing complex at the cytoplasmic membrane to the mitochondrial death machinery (Li et al., 1998; Luo et al., 1998). The full-length BID is inactive and present in the cytosolic fraction of living cells. Upon cleavage by Caspase 8, the COOH-terminal part of BID then translocates to mitochondria and is sufficient to trigger cytochrome c release in isolated mitochondria. BID demonstrates some very unique and important properties after cleavage by Caspase 8. In addition to the ability of truncated BID to translocate from cytosol to mitochondria, truncated BID has at least a 10-fold higher affinity toward BCL-X_L and is 100 times more efficient in inducing cytochrome c release from mitochondria compared to its full-length precursor (Li et al., 1998). Though BAX has also been shown to induce cytochrome c release both in vivo and in vitro (Jurgensmeier et al., 1998; Rosse et al., 1998), the cleaved BID is a much more potent cytochrome c–releasing factor than BAX (Luo et al., 1998). Mutagenesis studies have also shown that translocation of truncated BID onto mitochondria is independent of its BH3 domain (Luo et al., 1998). Due to its unique (or nonhomologous) sequence, BID has not been related to any known structures other than its BH3 domain. It remains to be a puzzle as to what conformational feature of BID allows it to acquire so much more potency in promoting cytochrome c release after Caspase 8 cleavage.

In this study, we have determined the solution structure of BID using NMR spectroscopy. It consists of eight α helices arranged in a compact fold in resemblance to transmembrane and pore-forming proteins of bacterial toxins, such as diphtheria toxin and the colicins, suggesting its potential to form selective ion channels on the mitochondrial membrane. Helices 6 and 7 are primarily hydrophobic and function as two central pillars, which are surrounded by six amphipathic helices. The structure of BID shows striking similarity to BCL-X_L despite the fact that the amino acid sequences of these two antagonists share only a 16-residue BH3 domain and are otherwise unrelated. Based on a structure of BCL-X_L–BAK BH3 peptide complex (Sattler et al., 1997) and the position of the BH3 domain–containing helix in BID, we modeled the interaction between BCL-X_L and the full-length BID. We also found that the four highly conserved hydrophobic residues of the BH3 domain that are responsible for heterodimerization are surface exposed in BID, suggesting their readiness to bind BCL-X_L. Additionally, we monitored the conformation change in BID during Caspase 8 cleavage and found that the overall structural integrity of BID is preserved after it is cleaved. Analyzing ^{15}N–^{1}H cross peak changes upon cleavage, conformational changes are localized and the role of Caspase 8 cleavage in the dramatic enhancement of proapoptotic activity of BID is elucidated. Finally, based on structure comparison of BID and BCL-X_L, along with the recent finding that BID can promote mitochondrial apoptosis independent of heterodimerization with BCL2 members, we propose that BID can induce mitochondrial damage through both BH3 domain–dependent and –independent mechanisms.

Results and Discussion

Structure Determination

The structure of full-length BID was defined by a total of 2202 NMR-derived distance constraints. For residues 42–78, no long-range NOEs were observed. The local sequential NOE patterns and transverse ^{15}N relaxation rates (data not shown) of this region are characteristic of an unstructured and flexible loop. Interestingly, BCL-X_L also has a long flexible loop (consisting of approximately 64 residues) near the N terminus (Muchmore et al., 1996). In addition to residues 42–78, the N-terminal 12 residues of BID, including Gly-1 and Ser-2 (which are part of the thrombin cleavage site in the GST fusion protein), are not defined in the structure. However, this is because the resonances of the amide protons of residues 3–9 were not observed due to either fast amide proton exchange with solvent (at pH 7.0) or conformational exchange on an intermediate time scale. In all other regions, the structure is well determined. The entire protein (including the loops) consists of 60% helices (Figure 1).

Overall, the structure determination employed the simple "local to global" strategy, which puts emphasis on stabilizing the local order prior to determination of the global fold. This approach is very efficient, especially for solving structures of helical proteins (see Experimental Procedures). First, the backbone NH resonances were rigorously confirmed by three pairs of triple-resonance experiments, selective ^{15}N labeling of Lys, Phe, Ser, Tyr, Leu, Val, Ile, and Ala residues, and sequential short-range NOEs. The ^{1}H and ^{13}C resonances of the side chains were determined by various TOCSY experiments. Second, helices were identified by both $^{13}C^{\alpha}$ chemical shift values (Wishart and Sykes, 1994) and NH(i)–HA (i − 3) and NH(i)–NH(i ± 1) NOE patterns. Additionally, using the short- and medium-range NOE patterns, some of the helix-turn-helix configurations were determined. The stabilization of local orders greatly reduced the conformation search space. Finally, the global fold was determined by identifying key NOEs between hydrophobic side chains. This was confirmed by analyzing 3D ^{15}N- and ^{13}C-dispersed NOESY and 2D homonuclear ^{1}H NOESY experiments. Complete structural statistics and root-mean-square deviation values are presented in Table 1. The precision of this structure can also be assessed from the dispersion of the 15 superimposed backbone traces shown in Figure 2A.

Structure Overview

The three-dimensional structure of BID is illustrated in Figure 2. Loops 1–12 and 43–77 are not displayed in the figure because they are completely disordered. The structured portion of BID consists of eight α helices arranged in a compact fold (Figures 2 and 5C). The primarily hydrophobic helices H6 and H7 are arranged in an antiparallel manner in the core of the protein. The

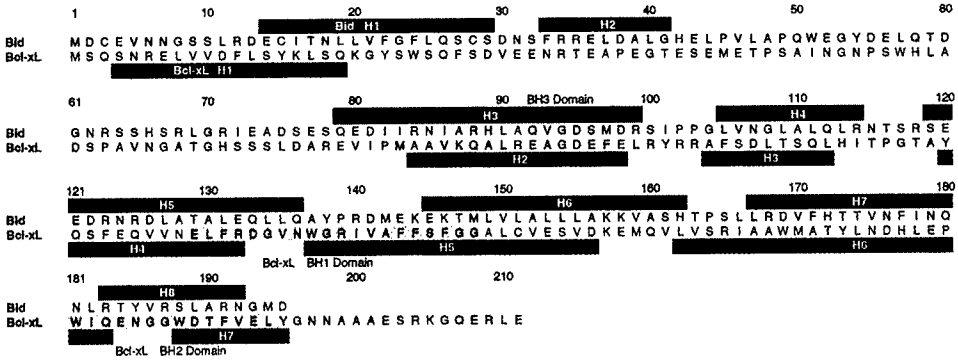

Figure 1. Amino Acid Sequences of BID and BCL-X_L Aligned at the BH3 Domains (Shaded in Yellow)

There is no sequence homology between the two proteins outside the BH3 domain. Red and blue bars indicate helices identified in BID and BCL-X_L, respectively. The BH1 and BH2 domains of BCL-X_L are shaded in light blue.

other six helices are amphipathic and packed around the two central helices. Helix H3 contains the BH3 domain and is fixed by hydrophobic contacts with helix H1 and helix H8. Structure comparison of BID and BCL-X_L (Figure 2C) shows extensive conformation homology between the two proteins (Muchmore et al., 1996) although their sequences are completely unrelated outside the 16-residue BH3 domain (Figure 1). The major difference between the two structures is that BID has an extra helix (H2) in its N-terminal region. Additionally, the flexible loop in BCL-X_L between the BH3 domain–containing helix (H2) and N-terminal helix (H1) is almost twice as long as that in BID. By matching the structurally homologous regions between these two molecules, we found that H1, H3, H4, H5, H6, H7, and H8 of BID correspond to H1, H2, H3, H4, H5, H6, and H7 of BCL-X_L, respectively (Figure 1).

The surface electrostatic potential of BID shown in Figure 3A does not reveal any unusually charged regions. However, BID has large hydrophobic patches on the surface (Figure 3B). Since BID and BCL-X_L are structurally similar, it is informative to compare their hydrophobic surfaces. Interestingly, four partially conserved hydrophobic residues of the BH3 domain (I82, I86, L90, and M97) are exposed in BID (Figures 1 and 3B), whereas those of BCL-X_L are buried (Figures 1 and 3C). As illustrated in Figure 3B, the surface of BID also has a large hydrophobic cleft formed by L105, Y140, V150, L151, and L154. This region remotely resembles the hydrophobic cleft (F105, L108, and L130) of BCL-X_L, which has been shown to bind BH3 death ligand (Sattler et al., 1997). However, biological implication of the BID hydrophobic cleft remains to be investigated. Thus far, neither BID homodimerization nor interaction between BID and BH3 ligand has been reported.

Structural Similarity to BCL-X_L Implies the Function of BID

Interaction between pro- and antiapoptotic members of the BCL2 family has long been considered a crucial mechanism for cell death induced by BAX-like members. However, multiple lines of recent evidence suggest that proapoptotic activities of BAX-like proteins are independent of the heterodimerization via the BH3 domain (discussed in Introduction). Studies have also shown that BID does not only function through heterodimerization with BCL2. A mutant of the truncated BID, which cannot bind BCL-X_L, can still target mitochondria and induce apoptosis very efficiently (H. L. and J. Y., unpublished results). In a separate study, Luo et al. showed that the BH3 mutant of the truncated BID (G94E) associated with mitochondria to the same extent as the wild type (Luo et al., 1998). On the other hand, heterodimerization may be important for the functions of BID. It has been proposed that heterodimerization with other prosurvival members of the BCL2 family is essential for the proapoptotic activity of the BH3 members (reviewed in Adams and Cory, 1998; Kelekar and Thompson, 1998). As the BH3 domain is the only homologous region that BID shares with other members of the family, heterodimerization would involve this domain. The above controversies may be resolved by the structural similarity between BID and BCL-X_L. Since the structure of BID is remarkably similar to BCL-X_L, we propose that BID is able to interact with mitochondria in a very similar way as to BCL-X_L and BAX, either by forming a selective ion channel or interacting with some unknown receptors on the membrane. BCL2 has been shown to bind the CED4-like portion of Apaf1, dependent on its N-terminal BH4 domain (helix H1 in Figures 1 and 2C), and thereby prevent the activation of Procaspase 9 (Hu et al., 1998; Pan et al., 1998). Since the truncated BID does not have the BH4 domain, one possible proapoptotic mechanism is that BID, upon cleavage by Caspase 8, can partially mimic BCL-X_L in interacting with mitochondria while not inhibiting proapoptotic molecules such as Apaf1. Indeed, this is in line with the previous finding, which was not well understood at the time, that cleavage of the N-terminal BH4 domain of BCL2 by Caspase 3 can convert BCL2 into a proapoptosis protein (Cheng et al., 1997). An equally possible mechanism would be that the cleaved BID can target the mitochondrial membrane and form selective ion channels that counter the effect of those formed by BCL-X_L.

Model for Heterodimerization between Full-Length BID and BCL-X_L

As mentioned previously, one of the proapoptotic mechanisms adopted by BAX and BH3 proteins is to bind BCL2 proteins and inhibit their antiapoptotic action via

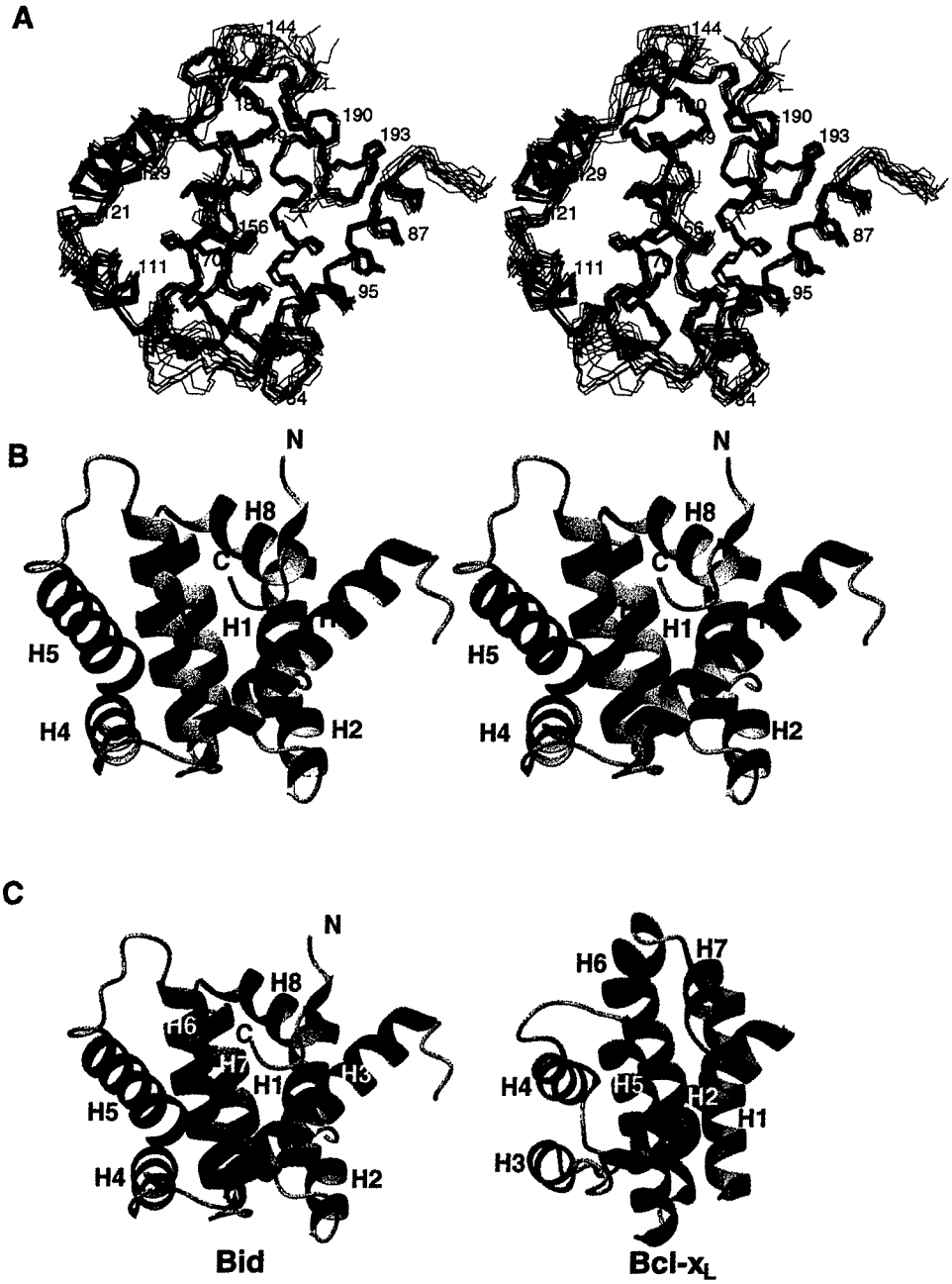

Figure 2. Solution Structure of BID

The flexible regions of BID (1–12 and 43–78) are not displayed.

(A) Stereoview of an ensemble of 15 out of 20 calculated structures representing the models with lowest energy (see Experimental Procedures). Only backbone atoms (N, C^{α}, C′) are shown.

(B) Ribbons stereodrawing of BID showing the eight helices, labeled H1–H8. This view emphasizes the position of the BH3 domain–containing H3 and the two hydrophobic helices H6 and H7.

(C) Ribbons drawings of BID (displayed in blue) and BCL-X_L (displayed in brown) showing the comparison of the two structures. The coordinates of BCL-X_L were obtained from the Protein Data Bank with the ID code 1MAZ. The figure was generated with MOLMOL (Koradi et al., 1996).

their BH3 "death ligands." This heterodimerization can either prevent BCL2 from interacting with Apaf1 or affect its ion channel formation on the mitochondria membrane that maintains the membrane potential (reviewed by Adams and Cory, 1998; Kelekar and Thompson, 1998). Now we know that BID and BAX members are structurally related and should interact with BCL2 in a similar fashion. The structure of BCL-X_L in complex with the BH3 amphipathic helix of BAK revealed that the insertion of the BH3 helix of BAK into the hydrophobic cleft of BCL-X_L (formed by its BH1 and BH2 domains) is a key event in the heterodimerization between death agonist and antagonist (Sattler et al., 1997). According to the structure and mutagenesis studies (Sattler et al., 1997),

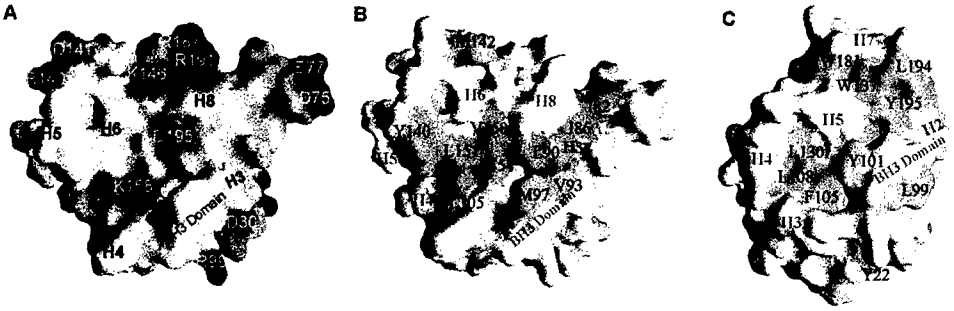

Figure 3. Surface Diagrams of BID and BCL-X_L

The BCL-X_L coordinates were obtained from the Protein Data Bank with ID code 1MAZ. In (A), the surface electrostatic potential is color coded such that regions with electrostatic potentials <-8 k_BT are red, while those $>+8$ k_BT are blue; k_B and T are the Boltzmann constant and temperature, respectively. In (B) and (C), surface-exposed hydrophobic residues, including Leu, Val, Ile, Met, Trp, Phe, and Tyr, are colored in light green. (A) Electrostatic potential surface of BID, showing no distinct charged regions. (B) Hydrophobic surface of BID formed primarily by residues in H6 and H3. (C) The elongated hydrophobic cleft of BCL-X_L to which the BAK BH3 peptide binds. This cleft is formed primarily by residues in H5 and H7. The figure was generated using GRASP (Nicholls et al., 1991).

four highly conserved hydrophobic side chains of the BAK BH3 helix point into the hydrophobic cleft of BCL-X_L and stabilize complex formation. These four residues are V74, L78, I81, and I85, and they are aligned with residues I86, L90, V93, and M97 of the BID BH3–containing helix (H3), respectively (Figure 1). Based on the homology model of BAK, derived from the structure of BCL-X_L, Sattler et al. found that the above four hydrophobic residues of the BAK BH3 domain point toward the interior of the BAK protein, making these residues unavailable to interact with BCL-X_L (Sattler et al., 1997). This is expected, since the corresponding residues are also buried in BCL-X_L (Figure 3C), which was the structural template for BAK modeling. As a result, the authors suggested that binding to BCL-X_L would necessitate a conformational change near the BAK BH3 helix to expose the hydrophobic surface of that helix. Furthermore, it was pointed out that such a conformational change is facilitated by the presence of the highly flexible loop preceding the BH3 helix.

Interestingly, residues I86, L90, V93, and M97 of the BID BH3 domain are surface exposed and ready to bind to a hydrophobic cleft. The surface representation of BID (Figure 3B) shows that these residues form an elongated hydrophobic patch on H3, adjacent to H8. Among these four residues, V93 and M97 completely point outward, whereas I86 and L90 are partially exposed and make contact with the hydrophobic residues on H8 (Figure 4A). Based on the information from the BCL-X_L–BAK peptide complex (Sattler et al., 1997), it is likely that I86 and L90 of BID are released from H8 and turn completely into the binding groove during heterodimerization. Additionally, the side chain of a highly conserved charged residue D95 (which corresponds to D83 of the BAK BH3 domain) leans toward the BID interior, yet is partially surface exposed. It is in a position to form a salt bridge with R100 and possibly R103 of BCL-X_L. This orientation is similar to that of D83 in the BCL-X_L–BAK complex structure. Since the BH3 helix of BID seems to be readily inserted into the hydrophobic cleft of BCL-X_L, we tested whether BID can be docked to BCL-X_L without any stereochemical conflict. By superimposing precisely the BH3 helix of BID and that of BAK (in complex with BCL-X_L), we were able to obtain a heterodimer model in which the binding surfaces of the two molecules complement each other reasonably well (Figure 4B). The model showed only minor stereochemical conflicts between the two molecules that can be readily eliminated by slight outward movement of BID H3 during the docking process.

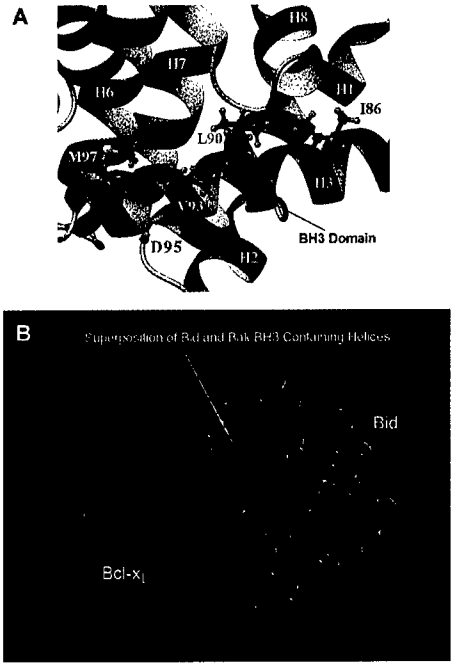

Figure 4. Model of the BID–BCL-X_L Heterodimer

(A) Ribbon diagram showing the BH3 domain of BID and its environment. The surface-exposed side chains of four highly conserved hydrophobic residues—I86, L90, V93, and M97—and the charged residue D95 are displayed.

(B) Overall view of the model for the BID–BCL-X_L heterodimer. The docking was performed using the InsightII program (Biosym, San Diego) by superimposing the BH3 domains of BAK and BID. Note that the red and blue BH3 helices of BAK and BID coincide almost completely. The rotational orientation around the BH3-helix axis was achieved by superimposing the conserved residues of the BH3 domains. The coordinates of BCL-X_L–BAK BH3 peptide complex were obtained from the Protein Data Bank (ID code 1BXL).

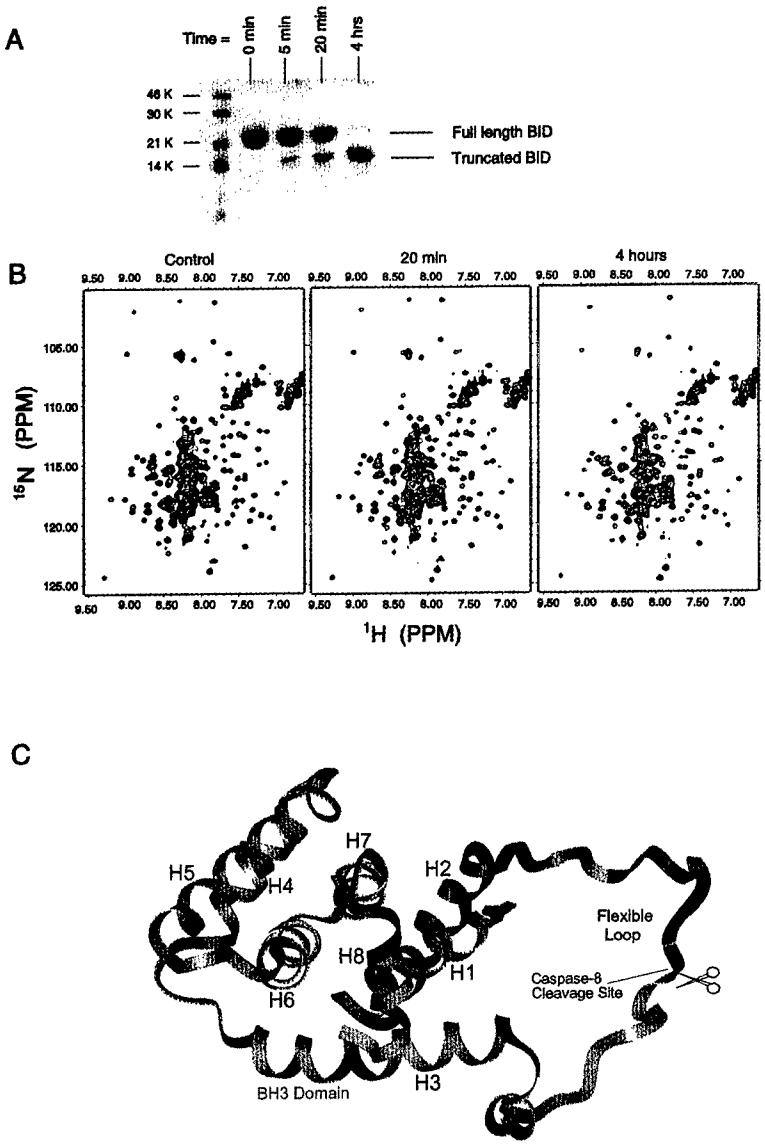

Figure 5. Monitoring the Conformation Change in BID during Caspase 8 Cleavage

The proteolytic reaction is initiated by mixing ^{15}N-labeled BID with unlabeled and active Caspase 8 at the ratio of 100:1.

(A) SDS-PAGE showing the fraction of cleaved BID. Four time points—0 min, 5 min, 20 min, and 4 hr—were recorded.

(B) ^{15}N–^{1}H HSQC spectrum of BID in the absence of Caspase 8 (control), BID after 20 min of Caspase 8 reaction, and BID after 4 hr of Caspase 8 reaction.

(C) Ribbon diagram of BID highlighting the residues whose local chemical environments are changed due to Caspase 8 cleavage. In this representation, residues of which NH chemical shift changes are greater than 0.1 and 0.02 ppm in ^{15}N and ^{1}H dimension, respectively (based on the spectra shown in [B]), are colored in red. Otherwise, they are illustrated in gray.

Mechanism of BID Activation by Caspase 8

Inasmuch as cleavage by Caspase 8 can greatly enhance the proapoptotic activity of BID, it has been hypothesized that such a dramatic activation is accompanied by major conformation changes after cleavage. To test this hypothesis, we monitored structural changes in BID during Caspase 8 proteolytic reaction using ^{15}N–^{1}H heteronuclear single quantum coherence correlation (HSQC) experiments (Bax et al., 1990; Cavanagh et al., 1996). The ^{15}N–^{1}H HSQC spectrum is characteristic of the protein conformation and is thus sensitive to structural changes. We initiated the proteolytic reaction by mixing full-length BID and active Caspase 8 at the ratio of 100:1 at room temperature. Then, ^{15}N–^{1}H HSQC spectra were recorded after 20 min and 4 hr. The fraction of cleaved BID at these two time points can be assessed from SDS-PAGE, shown in Figure 5A. The SDS-PAGE shows almost complete cleavage of BID after 4 hr of reaction (Figure 5A). The times above the HSQC spectra shown in Figure 5B are the times at which the individual experiment was started. Since each ^{15}N–^{1}H HSQC experiment took 1 hr and 10 min, the line shapes of the cross peaks that change upon cleavage are modulated in the spectrum started at 20 min. However, the spectrum recorded after 4 hr represents the fully cleaved product. Interestingly, the latter spectrum resembles very closely that of BID in the absence of Caspase 8 (the control) (Figure 5B), suggesting that the overall structural integrity of BID is preserved upon Caspase 8 cleavage. However, there are many small changes in resonance positions, which are a result of minor conformation changes, and can be easily traced in the spectra. Residues that showed significant chemical shift changes are highlighted in the ribbon drawing of BID (Figure 5C). As expected, the changes predominantly occurred in the loop region near the cleavage site, the N-terminal helices H1 and H2, H3 (containing the BH3 domain), H7, and H8. In the top view of the BID ribbon representation

shown in Figure 5C, it can be readily seen that H3, H7, and H8 all have close contacts with the N-terminal H1 and H2. Hence, small chemical shift changes are expected for these regions due to small rearrangements of H1 and H2 upon Caspase 8 cleavage.

The finding that the N-terminal domain remains intact at approximately the same position and orientation shows that the loop between H3 and H2 has no tension and plays no part in the folding of the eight helices in the uncleaved molecule. The unexpected result of this study is that the uncleaved and cleaved BID have approximately the same conformation. On the other hand, though the flexible loop is not important for the maintenance of BID structure, its cleavage has a profound effect on the proapoptotic activity. Upon cleavage, BID can target mitochondria and induce apoptosis independent of its BH3 domain (H. L. and J. Y., unpublished results). Additionally, truncated BID can bind approximately ten times stronger to BCL-X_L via its BH3 domain (Li et al., 1998). One possible mechanism for the activation of BID is that the N-terminal segment may serve as an internal inhibitor of proapoptotic activity. We propose that the proapoptotic activity of BID requires dissociation of the N-terminal segment including H1 and H2. While the N-terminal segment remains associated with the core of BID at the high concentrations used for the NMR experiment (Figure 5), at low cellular concentrations of BID this segment may detach after Caspase 8 cleavage and render the protein active. Even in the uncleaved BID, the N-terminal helices H1 and H2 may temporarily detach from the protein core, leading to some (although much lower) activity of the uncleaved protein.

The effect of Caspase 8 cleavage should be discussed with respect to the two models for the mechanism of BID function, formation of selective ion channels, like BCL-X_L and BAX, and/or inhibition of the interaction of BCL-X_L with Apaf1. Channel formation by BID could be promoted by Caspase 8 cleavage, since dissociation of the N-terminal segment would expose the hydrophobic face of helices H6 and H7 (Figure 5C). The two helices resemble closely the two central pore-forming helices H5 and H6 of BCL-X_L (Minn et al., 1997; Matsuyama et al., 1998), which have been considered important for channel formation. Figure 5C shows that dissociation of the N-terminal H1 and H2 can expose the central hydrophobic helices H6 and H7. Acquisition of channel-formation capabilities after cleavage may be the switch that enables the molecule to vigorously target mitochondria and promote cytochrome c release. However, the mechanism of cytochrome c release by pore formation is still unclear.

BID cleavage by Caspase 8 may also enhance heterodimerization with BCL-X_L and prevent the formation of the antiapoptotic complex between BCL-X_L and Apaf1. Dissociation of the N-terminal domain in BID is expected to loosen the contact of H3 and H8 with the protein core, and the H3 helix is less restricted to rearrange upon binding BCL-X_L. The putative binding site for BCL-X_L on helix H3 of BID and the contact area on H3 for the N-terminal helix H1 are on opposite faces of this H3 helix, and both interactions may have a competitive element. If cleaved BID is initially associated with the N-terminal domain, insertion of BH3 into the hydrophobic cleft of BCL-X_L could promote dissociation of H1 and H2. Thus, heterodimerization efficiency of the BH3 domain would depend on the local concentration of BCL-X_L and BID N-terminal domain. However, in full-length BID, the flexible loop can function as a chemical cross-link that can oppose heterodimerization with BCL-X_L by maintaining a much higher local concentration of the N-terminal domain.

Conclusion

We have determined the solution structure of BID, a proapoptosis member of the BCL2 regulatory family that has recently been established as a cross-talk agent for relaying the FAS/TNF apoptotic signal to the mitochondria death pathway. It consists of eight α helices arranged in a compact fold homologous to BCL-X_L. The structure of BID also revealed that the BH3 domain–containing helix is in a position ready for interaction with the hydrophobic cleft of BCL-X_L that has been shown to bind the BAK BH3 domain. Using the available structural data on the BCL-X_L–BAK BH3 peptide complex, we modeled the heterodimerization between BCL-X_L and the full-length BID by superimposing the BH3 domains of BAK and BID. Since BID becomes truly active in promoting cytochrome c release only after cleavage by Caspase 8, we monitored the conformation change in BID during Caspase 8 reaction using NMR spectroscopy. Analysis of the ^{15}N–^{1}H cross peaks of full-length and cleaved BID concluded that the overall structural integrity of BID is preserved after it is cleaved by Caspase 8. Additionally, based on the cleavage study, the role of Caspase 8 cleavage in the dramatic enhancement of proapoptotic activity of BID is elucidated. Although the BH3 domain of BID is critical for its heterodimerization with BCL-X_L, truncated BID is capable of targeting mitochondria and promoting mitochondria damage independent of its BH3 domain (Luo et al., 1998; H. L. and J. Y., unpublished results). In this study, we have provided a structural basis for truncated BID–induced mitochondrial damage. We propose that BID may have two modes of proapoptotic actions. First, BID can interact with proapoptotic members of the BCL2 family through their respective BH3 domains. We showed that although the full-length BID can interact reasonably well with BCL-X_L, cleavage by Caspase 8 and removal of H1 and H2 of BID may eliminate H1 as a competitive binder of the BH3 domain, making it more available for interacting with BCL-X_L. Second, BID also contains the structural motifs for pore formation and is potentially able to form selective ion channels similar to BAX and may promote apoptosis in a way other than inhibiting BCL2 proteins. Cleavage by Caspase 8 and dissociation of the N-terminal H1 and H2 expose the central hydrophobic helices H6 and H7, which remarkably resemble the two central pore-forming helices H5 and H6 of BCL-X_L (Minn et al., 1997; Matsuyama et al., 1998). The central hydrophobic helices H6 and H7 may be responsible for mitochondrial targeting after cleavage by Caspase 8 as well as potential pore-forming ability of BID. Overall, we

Table 1. Structural Statistics for the 15 Structures of Lowest Energy Obtained from 20 Starting Structures[a]

NOE distance restraints		
All	2202	
Intraresidue	610	
Interresidue	1592	
Sequential ($\|i - j\| = 1$)	760	
Medium	287	
i, i + 2	63	
i, i + 3	150	
i, i + 4	74	
Long ($\|i - j\| > 4$)	405	
Hydrogen bonds[b]	140	
Dihedral angle restraints		
ϕ ($C'_{(i-1)} - N_i - C_{\alpha i} - C'_i$)	93	
ψ ($N_i - C_{\alpha i} - C'_i - N_{(i+1)}$)	94	
$\chi 1$ ($N_i - C_{\alpha i} - C_{\beta i} - C_{\gamma 1 i}$ or $O_{\gamma 1 i}$)	74	
Ramachandrian plot[c]	Residues 13–44, 77–197	Secondary Structure
Most favorable region	70.2	81.1
Additionally allowed region	21.7	15.4
Generously allowed region	7.3	3.3
Disallowed region	0.8	0.2
Average rms deviations from experimental distance restraints (Å) all (2102)		0.044 ± 0.001
Average rms deviations from experimental dihedral restraints (°) all (261)		0.32 ± 0.04
Average rms deviations from idealized covalent geometry		
Bonds (Å)		0.003 ± 0.0001
Angles (°)		0.48 ± 0.006
Impropers (°)		0.42 ± 0.010
Average rms deviations of atomic coordinates between 15 structures[d]	Residues 13–44, 77–197	Secondary Structure
Backbone (Å)	0.92	0.54
Heavy atoms (Å)	1.44	0.93

[a] None of these structures exhibited distance violations greater than 0.4 Å or dihedral angle violations greater than 5°.
[b] During structure calculation, hydrogen bond restraints were added only for α helices, identified based on backbone $^{13}C\alpha$ resonances (Wishart and Sykes, 1994) and NH(I)–HA(I − 3, I − 4) NOE observed in the 3D ^{15}N-NOESY-HSQC spectrum.
[c] The program PROCHECK_nmr (Laskowski et al., 1993) was used to assess the quality of the structures.
[d] The precision of the atomic coordinates is defined as the average rms differences between the 15 final calculated structures and the mean coordinates.

propose that although there is only very limited sequence homology between BID and BAX, BID acts very similarly to BAX and may have multiple modes of action in inducing mitochondrial damage.

The conformational similarity between BID and BCL-X_L is rather surprising, since the two proteins are unrelated in their amino acid sequences. This has been independently shown by McDonnell et al. (1999 [this issue of *Cell*]), who have solved the BID structure at 45°C. However, this phenomenon was also observed for proteins involved in caspase recruitment. The FAS death domain (DD), FADD death effector domain (DED), and caspase recruitment domain (CARD) are unrelated in sequence yet adopt the similar six-helix bundle conformations (Huang et al., 1996; Chou et al., 1998; Eberstadt et al., 1998). The recurrence of this phenomenon of different sequences yielding similar structures suggests that apoptosis is an ancient process that involves a limited number of evolutionarily highly conserved structural motifs. In order for them to construct an intricate network of regulatory pathways, a high degree of specificity must be employed. For instance, BCL-X_L, BID, and BAX are structurally similar yet functionally nonredundant. Still, little is known about the detailed molecular mechanisms that allow them to take different roles in apoptosis.

Experimental Procedures

Expression and Purification of BID

Human full-length BID gene was amplified by PCR from EST cDNA clone 52055 using primers HL176 (5′ CCGGATCCATGGACTGTGAG GTCAAC) and HL178 (5′ GGGGATCCCTGAGTCAGTCCATCCCATTT CTG) and then cloned into the BamHI site of pGEX-2T vector. BID was expressed in *Escherichia coli* with GST fused at the N terminus. The transformed cells were grown in either LB-rich media (for unlabeled protein) or M9-minimal media (for labeled protein). For isotope labeling, the M9 media were substituted with ^{15}N-labeled ammonia (1 g l^{-1}) or ^{13}C glucose (2 g l^{-1}). For triple-resonance experiments, uniformly ^{15}N, ^{13}C, ^{2}H-labeled protein was prepared by growing the cells in 90% D_2O with ^{15}N-labeled ammonia and ^{13}C glucose. A 50% deuterated and ^{15}N, ^{13}C-labeled sample was prepared by growing the cells in 50% D_2O with ^{15}N ammonia and ^{13}C glucose. For selective amino acid labeling, the plasmid was transformed into DL39 cell line (cell that lacks aminotransferase) to minimize cross labeling between different amino acids. Selective ^{15}N labeling was done by growing the cells in M9 media supplemented with selected ^{15}N-labeled amino acids.

After cell lysis, the GST-fusion recombinant protein was first separated from other *E. coli* proteins by GST affinity chromatography at pH 7 and then cleaved off GST with thrombin (Biotech Pharmacia). The eluted BID was purified to homogeneity using gel filtration (Sephadex G-50). The identity of the protein was confirmed by N-terminal sequencing, amino acid composition analysis, and SDS-PAGE. NMR samples contained 1 mM protein in 20 mM Tris (pH 7.0) and 5 mM NaCl in H_2O/D_2O (9/1) or D_2O. For the homonuclear NOESY experiment, the sample contained 1 mM protein in 50 mM

$NaPO_4$ (pH 7.0) in D_2O. The NMR sample used for monitoring Caspase 8 cleavage was prepared by mixing 1 mM ^{15}N-labeled BID with unlabeled Caspase 8 at the ratio of 100:1.

NMR Spectroscopy

All NMR spectra were acquired at 25°C on Varian Unity 500, Varian UnityPlus 500, Bruker 600, or Varian UnityPlus 750 spectrometers. For assignment of the backbone ^1H, ^{13}C, and ^{15}N resonances, three pairs of triple-resonance experiments were recorded using uniformly ^{15}N, ^{13}C-labeled and 90% deuterated protein in H_2O. These are [HNCA, HN(CO)CA], [HNCO, HN(CA)CO], and [HN(CA)CB, HN(COCA)CB] (for overviews, see Clore and Gronenborn, 1993; Yamazaki et al., 1994; Matsuo et al., 1996a, 1996b). $^{13}C^{\beta}$ decoupling was used in HNCA and HN(CO)CA for higher $^{13}C^{\alpha}$ resolution and better signal sensitivity (Matsuo et al., 1996b). In addition, amino acid–selective ^{15}N labeling of Lys, Phe, Ser, Tyr, Val, Leu, Ile, and Ala was used to confirm the sequential assignment of amide protons. Side-chain proton resonances were mostly assigned using 3D Cbd-HCCH-TOCSY (Clore and Gronenborn, 1994; Matsuo et al., 1997) and 3D ^{15}N-dispersed TOCSY-HSQC spectra, recorded using uniformly ^{15}N, ^{13}C-labeled protein in D_2O and uniformly ^{15}N-labeled protein in H_2O, respectively. The assignment of aromatic side chains was accomplished using homonuclear TOCSY and NOESY experiments, acquired with the nonlabeled protein in D_2O. Stereospecific assignment of methyl groups of Val and Leu residues was obtained from ^{13}C-HSQC spectrum of a 10% ^{13}C-labeled protein (Szyperski et al., 1992). Transverse ^{15}N relaxation rates were measured with experiments as described by Peng and Wagner (1992) and Farrow et al. (1994).

Distance restraints between amide protons and side chains were obtained from two ^{15}N-dispersed NOESY spectra, acquired with mixing times of 60 and 120 ms. Long-range distance restraints between side chains (especially those of Val, Leu, and Ile) were obtained from a ^{13}C-dispersed NOESY experiment with a mixing time of 100 ms. NOE connectivities between aromatics and from aromatics to nonaromatic side chains were assigned with the combination of homonuclear 2D NOESY and ^{13}C-dispersed NOESY spectra. NOE distance restraints used for the structure calculations are summarized in Table 1. Hydrogen bond distance restraints were imposed only for the helical region, identified on the basis of $^{13}C^{\alpha}$ chemical shift values (Wishart and Skyes, 1994) and NH(i)-HA(i − 3, i − 4) NOE cross peaks. The backbone torsion angles ϕ and ψ were obtained using a method for measuring proton splitting in ^{15}N-HSQC spectrum by J doubling (del Rio-Portilla et al., 1994). The torsion angles $\chi 1$ of side chains in helical regions were restrained within the ranges found in refined crystal structure using the rotamer libraries of Dunbrack and Karplus (1993).

Structure calculations were performed following simulated annealing protocols of Nilges et al. (1988) using X-PLOR 3.851 (Brünger, 1993) on R10000 Indigoll Silicon Graphics work stations. Out of 20 starting structures, 19 had no violations larger than 0.4 Å or dihedral angle violations greater than 5°. The 15 structures with the lowest energy were selected for display (superimposed in Figure 2A). Structures were displayed and analyzed using the InsightII program (Biosym, San Diego), GRASP (Nicholls et al., 1991), MOLMOL (Koradi et al., 1996), and PROCHECK_nmr (Laskowski et al., 1993). The structural statistics are presented in Table 1.

Acknowledgments

We thank Greg Heffron for help with the use of spectrometers and Alexey Lugovskoy for kind assistance in making the figures. This research was supported in part by a grant from the NIH (GM 38608 and GM 47467) to G. W., a grant from the Breast Cancer Program of the US Army to J. Y., and a postdoctoral fellowship to H. L. Acquisition and maintenance of spectrometers and computers used for this work were supported by NSF (MCB 9527181) and the Harvard Center for Structural Biology and the Giovanni Armenise-Harvard Foundation for Advanced Scientific Research.

Received December 24, 1998; revised January 20, 1999.

References

Adams, J.M., and Cory, S. (1998). The Bcl-2 protein family: arbiters of cell survival. Science *281*, 1322–1326.

Bax, A., Ikura, M., Kay, L.E., and Torchia, D.A. (1990). Comparison of different modes of two dimensional reverse correlation NMR for the study of proteins. J. Magn. Reson. *86*, 304–318.

Boldin, M.P., Goncharov, T.M., Goltsev, Y.V., and Wallach, D. (1996). Involvement of MACH, a novel MORT1/FADD-interacting protease, in Fas/APO-1- and TNF receptor–induced cell death. Cell *85*, 803–815.

Brünger, A.T. (1993). XPLOR Version 3.1 (New Haven, CT: Yale University Press).

Cavanagh, J., Fairbrother, W.J., Palmer, A.G., III, and Skelton, N.J. (1996). Protein NMR Spectroscopy (San Diego, CA: Academic Press).

Cheng, E.H., Kirsch, D.G., Clem, R.J., Ravi, R., Kastan, M.B., Bedi, A., Ueno, K., and Hardwick, J.M. (1997). Conversion of Bcl-2 to a Bax-like death effector by caspases. Science *278*, 1966–1968.

Chou, J.J., Matsuo, H., Duan, H., and Wagner, G. (1998). Solution structure of the RAIDD CARD and model for CARD/CARD interaction in Caspase-2 and Caspase-9 recruitment. Cell *94*, 171–180.

Clore, G.M., and Gronenborn, A.M. (1994). Multidimensional heteronuclear nuclear magnetic resonance of proteins. Methods Enzymol. *239*, 349–363.

Cosulich, S.C., Worrall, V., Hedge, P.J., Green, S., and Clarke, P.R. (1997). Regulation of apoptosis by BH3 domains in a cell-free system. Curr. Biol. *7*, 913–920.

del Rio-Portilla, F., Blechta, V., and Freeman, R. (1994). Measurement of poorly-resolved splittings by J-doubling in the frequency domain. J. Magn. Reson. *A111*, 132–135.

Dunbrack, R., and Karplus, M. (1993). Backbone-dependent rotamer library for proteins. Application to side-chain prediction. J. Mol. Biol. *230*, 543–574.

Eberstadt, M., Huang, B., Chen, Z., Meadows, R.P., Ng, S., Zheng, L., Lenardo, M.J., and Fesik, S.W. (1998). NMR structure and mutagenesis of the FADD (Mort1) death-effector domain. Nature *392*, 941–945.

Farrow, N.A., Muhandiram, R., Singer, A.U., Pascal, S.M., Kay, C.M., Gish, G., Shoelson, S.E., Pawson, T., Forman-Kay, J.D., and Kay, L.E. (1994). Backbone dynamics of a free and a phosphopeptide-complexed Src homology 2 domain studied by ^{15}N NMR relaxation. Biochemistry *33*, 5984–6003.

Green, D.R. (1998). Apoptotic pathways: the roads to ruin. Cell *94*, 695–698.

Hu, Y., Benedict, M.A., Wu, D., Inohara, N., and Nunez, G. (1998). Bcl-x_L interacts with Apaf-1 and inhibits Apaf-1-dependent caspase-9 activation. Proc. Natl. Acad. Sci. USA. *95*, 4386–4391.

Huang, B., Eberstadt, M., Olejniczak, E.T., Meadows, R.P., and Fesik, S.W. (1996). NMR structure and mutagenesis of the FAS (APO-1/CD95) death domain. Nature *384*, 638–641.

Jurgensmeier, J.M., Xie, Z., Deveraux, Q., Ellerby, L., Bredesen, D., and Reed, J.C. (1998). Bax directly induces release of cytochrome c from isolated mitochondria. Proc. Natl. Acad. Sci. USA *95*, 4997–5002.

Kelekar, A., and Thompson, C.B. (1998). Bcl-2-family proteins: the role of the BH3 domain in apoptosis. Trends Cell Biol. *8*, 324–329.

Kluck, R.M., Bossy-Wetzel, E., Green, D.R., and Newmeyer, D.D. (1997). The release of cytochrome c from mitochondria: a primary site for bcl-2 regulation of apoptosis. Science *275*, 1132–1136.

Knudson, C.M., and Korsmeyer, S.J. (1997). Bcl-2 and Bax function independently to regulate cell death. Nat. Genet. *16*, 358–363.

Koradi, R., Billeter, M., and Wüthrich, K. (1996). MOLMOL: a program for display and analysis of macromolecular structures. J. Mol. Graph. *14*, 51–55.

Kuwana, T., Smith, J.J., Muzio, M., Dixit, V., Newmeyer, D.D., and Kornbluth, S. (1998). Apoptosis induction by Caspase-8 is amplified through the mitochondrial release of cytochrome c. J. Biol. Chem. *273*, 16589–16594.

Laskowski, R.A., MacArthur, M.W., Moss, D.S., and Thornton, J.M. (1993). PROCHECK: a program to check the stereochemical quality of protein structures. J. Appl. Crystallogr. *26*, 283–291.

Li, P., Nijhawan, D., Budihardjo, I., Srinivasula, S.M., Ahmad, M.,

Alnemri, E.S., and Wang, X. (1997). Cytochrome c and dATP-dependent formation of Apaf-1/Caspase-9 complex initiates an apoptotic protease cascade. Cell *91*, 479–489.

Li, H., Zhu, H., Xu, C.-J., and Yuan, J. (1998). Cleavage of BID by Caspase 8 mediates the mitochondrial damage in the Fas pathway of apoptosis. Cell *94*, 491–501.

Luo, X., Budihardjo, I., Zou, H., Slaughter, C., and Wang, X. (1998). Bid, a Bcl2 interacting protein, mediates cytochrome c release from mitochondria in response to activation of cell surface death receptors. Cell *94*, 481–490.

Matsuo, H., Li, H., and Wagner, G. (1996a). A sensitive HN(CA)CO experiment for deuterated proteins. J. Magn. Reson. B *110*, 112–115.

Matsuo, H., Kupce, E., Li, H., and Wagner, G. (1996b) Increased sensitivity in HNCA and HN(CO)CA experiments by selective C^{β} decoupling. J. Magn. Reson. B *113*, 91–96.

Matsuo, H., Li, H., McGuire, A.B., Fletcher, C.M., Gingras, A., Sonenberg, N., and Wagner, G. (1997). Structure of translation factor eIF4E bound to m^7GDP and interaction with 4E-binding protein. Nat. Struct. Biol. *4*, 717–724.

Matsuyama, S., Schendel, S.L., Xie, Z., and Reed, J.C. (1998). Cytoprotection by Bcl-2 requires the pore-forming $\alpha5$ and $\alpha6$ helices. J. Biol. Chem. *273*, 30995–31001.

McDonnell, J.M., Fushman, D., Milliman, C.L., Korsmeyer, S.J., and Cowburn, D. (1999). Solution structure of the proapoptotic molecule BID: a structural basis for apoptotic agonists and antagonists. Cell *96*, this issue, 625–634.

Minn, A.J., Velez, P., Schendel, S.L., Liang, H., Muchmore, S.W., Fesik, S.W., Fill, M., and Thompson, C.B. (1997). Bcl-x_L forms an ion channel in synthetic lipid membranes. Nature *385*, 353–357.

Muchmore, S.W., Sattler, M., Liang, H., Meadows, R.P., Harlan, J.E., Yoon, H.S., Nettesheim, D., Chang, B.S., Thompson, C.B., Wong, S.L., et al. (1996). X-ray and NMR structure of human Bcl-x_L, an inhibitor of programmed cell death. Nature *381*, 335–341.

Muzio, M., Chinnaiyan, A.M., Kischkel, F.C., O'Rourke, K., Shevchenko, A., Ni, J., Scaffidi, C., Bretz, J.D., Zhang, M., Gentz, R., et al. (1996). FLICE, a novel FADD-homologous ICE/CED-3 like protease, is recruited to the CD95 (Fas/APO-1) death-inducing signaling complex. Cell *85*, 817–827.

Muzio, M., Stockwell, B.R., Stennicke, H.R., Salvesen, G.S., and Dixit, V.M. (1998). An induced proximity model for caspase-8 activation. J. Biol. Chem. *273*, 2926–2930.

Nicholls, A., Sharp, K.A., and Honig, B. (1991). Protein folding and association: insights from the interfacial and thermodynamic properties of hydrocarbons. Proteins *11*, 281–296.

Nilges, M., Clore, G.M., and Gronenborn, A.M. (1998). Determination of three-dimensional structures of proteins from interproton distance data by dynamical simulated annealing from a random array of atoms. FEBS Lett. *239*, 129–136.

Pan, G., O'Rourke, K., and Dixit, V.M. (1998). Caspase-9, Bcl-x_L, and Apaf-1 form a ternary complex. J. Biol. Chem. *273*, 5841–5845.

Peng, J.W., and Wagner, G. (1992). Mapping of spectral density functions using heteronuclear NMR relaxation measurements. J. Magn. Reson. *98*, 308–332.

Rosse, T., Olivier, R., Monney, L., Rager, M., Conus, S., Fellay, I., Jansen, B., and Bomer, C. (1998). Bcl-2 prolongs cell survival after Bax-induced release of cytochrome c. Nature *391*, 496–499.

Sattler, M., Liang, H., Nettesheim, D., Meadows, R.P., Harlan, J.E., Eberstadt, M., Yoon, H.S., Shuker, S.B., Chang, B.S., Minn, A.J., et al. (1997). Structure of Bcl-x_L-Bak peptide complex: recognition between regulators of apoptosis. Science *275*, 983–986.

Scaffidi, C., Fulda, S., Srinivasan, A., Friesen, C., Li, F., Tomaselli, K.J., Debatin, K.M., and Krammer, P.H. (1998). Two CD95 (APO-1/Fas) signaling pathways. EMBO J. *17*, 1675–1687.

Szyperski, T., Neri, D., Leithing, B., Otting, G., and Wüthrich, K. (1992). Support of 1H NMR assignments in proteins by biosynthetically directed fractional ^{13}C-labeling. J. Biomol. NMR *2*, 323–334.

Wang, K., Gross, A., Waksman, G., and Korsmeyer, S.J. (1998). Mutagenesis of the BH3 domain of BAX identifies residues critical for dimerization and killing. Mol. Cell. Biol. *18*, 6083–6089.

Wishart, D.S., and Sykes, B.D. (1994). The ^{13}C chemical-shift index: a simple method for the identification of protein secondary structure using ^{13}C chemical-shift data. J. Biomol. NMR *4*, 171–180.

Yamazaki, T., Lee, W., Arrowsmith, C.H., Muhandiram, D.R., and Kay, L.E. (1994). A suite of triple resonance NMR experiments for the backbone assignment of ^{15}N, ^{13}C, ^{2}H labeled proteins with high sensitivity. J. Am. Chem. Soc. *116*, 11655–11666.

Yang, J., Liu, X., Bhalla, K., Kim, C.N., Ibrado, A.M., Cai, J., Peng, T.I., Jones, D.P., and Wang, X. (1997). Prevention of apoptosis by bcl-2 release of cytochrome c from mitochondria blocked. Science *275*, 1129–1132.

Yang, X., Chang, H.Y., and Baltimore, D. (1998). Autoproteolytic activation of pro-caspases by oligomerization. Mol. Cell *1*, 319–325.

Protein Data Bank ID Code

The coordinates for the human BID structure were deposited in the Protein Data Bank under ID code 2bid.